Supporting Information for the manuscript:

Water consumption footprint and land requirements of large-scale alternative diesel and jet fuel production

Mark D. Staples, Hakan Olcay, Robert Malina, Parthsarathi Trivedi, Matthew N. Pearlson, Kenneth Strzepek, Sergey V. Paltsev, Christoph Wollersheim, Steven R.H. Barrett

52 pages total (excluding cover page):

26 Figures

18 Tables

S1 GAEZ Model

This analysis assesses agricultural resources and potential using the Agro-Ecological Zones (AEZ) methodology developed at The International Institute for Applied Systems Analysis (IIASA) and the Food and Agriculture Organization of the United Nations (FAO). Global Agro-Ecological Zones (GAEZ) v3.0 provides a major update of data and extension of the methodology of the release of GAEZ in 2002.[1] We use GAEZ v3.0 to estimate biomass yields, green water, and blue water consumption requirements. The data sources used by GAEZ v3.0 are described below, and the inputs and outputs of GAEZ v3.0 are shown in Figure S1.

GAEZ uses geo-referenced global climate, soil and terrain data, and combines it into a land resources database. The database is assembled for a global grid with 5 arc-minute and 30 arc-second resolution. Agronomical climate resource inventories are compiled using precipitation, temperature, wind speed, sunshine hours and relative humidity. Crop-specific limitations are identified, under assumed input and management conditions, using prevailing climate, soil and terrain resources. GAEZ provides maximum potential and agronomically attainable crop yields defined by: agricultural production system, water supply system, level of input, and management circumstances.[2]

S1.1 Yield and water use calculations

GAEZ uses solar irradiation and temperature regimes to calculate the maximum attainable biomass yield, rainfed crop water balances, and optimum crop calendars. Crop water balances are used to estimate actual crop evapotranspiration, accumulated crop water deficit during the growth cycle, irrigation water requirements for irrigated conditions, and the corresponding rainfed and irrigated biomass yields. GAEZ takes into account yield reductions due to agro-climatic constraints, soil and terrain limitations; climate data;[3] soil data;[4] elevation, terrain slope and aspect data;[5] and land cover data.[6–14] This model description is adapted from Fischer et al.[1]

S1.2 Model validation

The stepwise agro-ecological suitability analysis procedure used by the GAEZ model is outlined in Fischer et al. (2002) on pages 60-64,[15] and a brief confirmation of the results is discussed on page 64. In addition, the GAEZ model has been verified both internally by IIASA and by FAO's Economic

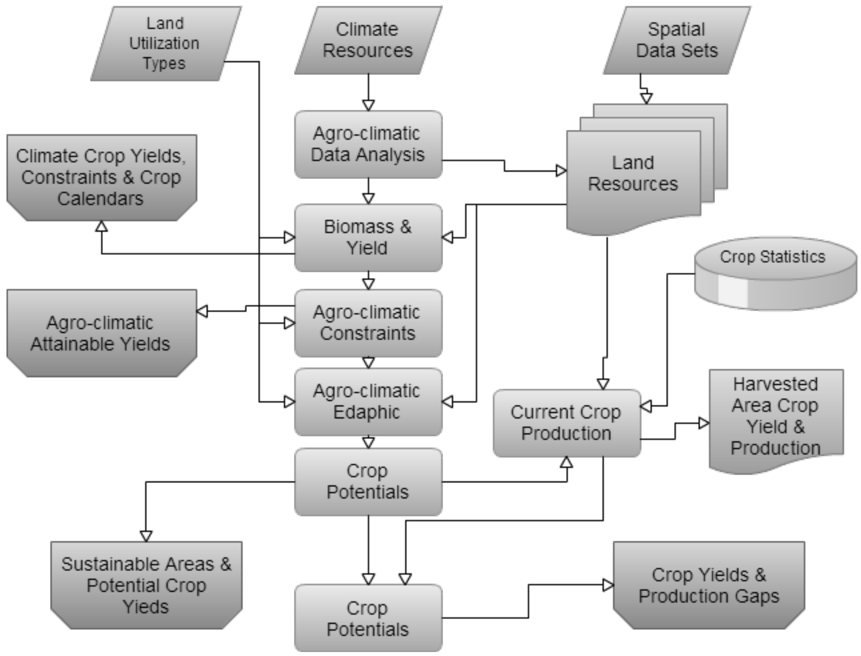

Figure S1: Structure and data integration of GAEZ v3.0 (module I-VII). Adapted from Fischer et al.[1]

and Social, and Agricultural Departments, and the crop yields and distributions have been verified against national agricultural statistics.[1,16] Derivatives of the GAEZ model, such as M-GAEZ, have been externally verified for accuracy.[17] The Global Environmental Change and Food Systems (GECAFS) project compared the GAEZ model against others with similar objectives.

Notable projects and work containing AEZ assessments include Wackernagel et al.[18], and the Comprehensive Assessment of Water Management in Agriculture (CAWMA).[19] The GAEZ model was also used by the Intergovernmental Panel on Climate Change (IPCC) for the Fourth Assessment Report (AR4) for assessing food security under soil, terrain and climate constraints.

It is important to note that GAEZ estimates the agro-ecological and climatically maximum attainable yields, and does not provide a one-for-one prediction of actual yields. Therefore, there may be some discrepancy between the agricultural productivity predicted by GAEZ and actual yield data. This dicrepancy, termed “yield gap,” is discussed in detail in Deininger et al.[20] Our analysis makes use of the maximum attainable yields calculated by GAEZ, under an assumption of “intermediate” level inputs.

S1.3 Green and blue water consumption data

Green water and blue water consumption data for biomass cultivation is calculated from rainfed and irrigated evapotranspiration (ET) data.[1] This data was extracted under an assumption of “intermediate” level inputs for biomass culativation, as contained in the GAEZ model. Rainfed (actual) ET represents green water consumption of vegetation growth, via evapotranspiration, under an assumption of no applied irrigation water. Irrigated (potential) ET represents green and blue water consumption via evapotranspiration under an assumption of irrigation water applied to maximize biomass yield. By taking the difference of irrigated ET and rainfed ET (that is, ET additional to rainfed ET, and attributable to irrigation), we estimate the blue water consumption requirements of irrigation in order to maximize biomass yield.

For more detail on the methodology employed by GAEZ to calculate crop ET, including information on agro-climatic and biomass yield calculations, please refer to Sections 3 and 4 (pg. 17-36 and 37-47) of Fischer et al.[1]

S2 Pathway information

S2.1 Primary energy carrier data

The water intensities of primary energy carriers used in this analysis are based on Gleick.[21] This the most apporpriate data source for this analysis because other possible data sources, such as the EcoInvent of SimaPro databases, tabulate water withdrawl rather than consumption, which is required for our analysis. Furthermore, subsequent studies on the water consumption of primary energy carrier production, such as King & Webber and Gerbens-Leenes et al., are based on the data reported in Gleick.[21–23]

The water intensity value for coal used for this analysis (0.164 $\frac{l}{MJ}$) is taken directly from Gleick.[21] In order to reflect current technology deployment for the extraction of natural gas, we calculate a weighted average of water consumption of conventional extraction from Gleick, and hydraulic fracturing from King & Webber.[21,23] The proportion of natural gas produced in the US using hydraulic fracturing was calculated from EIA data from 2011.[24]

$$\begin{gathered}\left(0.109\tfrac{l}{MJ}\right)^{21} + \\ \left(0.0067\frac{gal}{SCF}\right)^{23} * \left(\tfrac{13.7}{23.0}\right)^{24} * \tfrac{1}{983}\ \frac{SCF}{BTU} * 3587.9\ \frac{l/MJ}{gal/BTU} \\ = 0.124\ \frac{l}{MJ}\end{gathered}$$

Finally, the petroleum, diesel and residual oil values (0.127, 0.153 and 0.166 $\frac{l}{MJ}$, respectively) were calculated using the procedure outlined in Section S2.2.

S2.2 Conventional MD

The conventional MD pathway lifecycle includes crude oil recovery, crude oil transportation, refining of crude oil to MD, and MD transportation and distribution.

Crude oil is a mixture of hydrocarbons and other organic compounds that is extracted by drilling wells into underground geological reservoirs. The crude is drawn from the wells in the form of liquid, and is accompanied by gas and produced water (PW). Different technologies are used to extract crude oil from wells as the wells age. Generally, a new oil well has sufficient reservoir pressure to carry the mixture of oil, gas and PW up to the surface. This naturally occurring type of extraction is called primary recovery. Over time, as material is removed from the reservoir, the reservoir pressure, and the efficacy of primary recovery, drops. Secondary recovery techniques are then applied, which involve injecting water (recycled PW, saline or fresh water) into the reservoir to maintain reservoir pressure and continue to push crude oil to surface. This technique, also known as water flooding, is only efficient for a certain period of time, as the less viscous water and surface tension eventually causes the more viscous oil to be trapped in the reservoir rock. Tertiary oil recovery, which is also called enhanced oil recovery (EOR), typically makes use of either CO_2 and surfactant injection to reduce the surface tension, or of steam and micellar polymer (a type of surfactant) injection to reduce viscosity contrast. A third EOR technique is called forward combustion, during which a flame front created by combustion of the deposits with continuous air injection propagates towards the well, which decreases the viscosity of the oil to be extracted due to high temperatures.[25] Forward combustion and other EOR technologies account for only 2% of total EOR.

67% of US oil production relies on crude oil extracted from onshore wells, and this analysis assumes that all secondary and tertiary recovery is taking place in onshore wells.[26] If secondary recovery was performed in offshore wells, seawater would most likely be used, therefore the assumption of secondary extraction taking place onshore results in a higher estimate of fresh water use.

The amount of water used during extraction depends on the technology used. The values range from 0.21 [l_{water}/l_{crude}] recovered for the case of primary recovery, to 343 [l_{water}/l_{crude}] for EOR using micellar polymer injection.[26] For secondary recovery and EOR, water consumption is primarily associated with injected water that cannot be recycled or re-used. For primary recovery, however, water is used during drilling for mixing the drilling mud, and during recycled water (RW) treatment. Table S1 shows the amount of water used by each technology along with the technology shares for oil extraction. A technology-weighted average water consumption value of 8 [l_{water}/l_{crude}], excluding re-injection, is obtained from all the major primary, secondary and tertiary recovery systems.[26]

The blue water consumption of crude oil extraction varies mainly according to the produced water re-injection technologies employed in each Petroleum Administration for Defense District (PADD), as does the amount of oil produced and the number of wells being operated. CONUS is divided into five PADDs, three of which (PADD II, III and V) account for 81% of US refinery products and 90% of onshore crude oil production.[26] This analysis uses a weighted average of the values for PADDs II, III and V as a proxy for the US average. Table S2 presents the average volume of PW that is re-injected during oil recovery for PADDs II, III and V. The net water needed, also given in the table, indicates the net amount of water consumed during oil extraction and recovery. An average blue water consumption of 3.3 [l_{water}/l_{crude}] is estimated for the US.[26]

The processes that use water in a typical refinery include the cooling tower, crude distillation unit and fluid catalytic cracker (FCC). Steam and cooling operations in a refinery make up about 96% of the refinery water consumption.[26] Figure S2 shows the water flow in a typical North American

Table S1: Oil production, water injection and technology share of various recovery technologies from Wu et al.[26]

Recovery technology	Oil prod. [bpd]	Oil prod. [Mgal/d]	Tech. share [%]	Water inj. [Mgal/d]	Spec. water consump. [l_{water}/l_{crude}]
CO_2 miscible	234 315	9.8	10.9	127.9	13
CO_2 immiscible	2 698	0.1	0.1	1.5	13
Steam	286 668	12.0	5.5	65	5.4
Combustion	13 260	0.6	0.1	1.1	1.9
Other EOR[a]	112 276	4.7	3.5	40.9	8.7
Sec. water flood	2 589 000	108.7	79.7	933	8.6
Primary recovery	227 783	9.6	0.2	2	0.2
Total	3 466 000	145.6	100	1 171	-
				Weighted av.	8.0

[a]Data on water use are not publicly available for "other EOR" technologies, including hydrocarbon miscible/immiscible, hot-water flooding, and nitrogen injection. Average values for CO_2, steam and air combustion EOR is assumed for the "other EOR" technologies for which data is not available.

Table S2: Water use during oil extraction and recovery from Wu et al.[26]

PADD	Technology-weighted average water injection	PW re-injected	Net water req'd.
		[l_{water}/l_{crude}]	
II	8.0	5.9	2.1
III		5.7	2.3
V		2.6	5.4

refinery. Approximately 1.5 liters of water are consumed for every liter of crude oil processed in an oil refinery.[26]

GREET 2011[27] is used as the reference for assumptions associated with transportation of crude oil, residual oil, diesel fuel and conventional jet fuel. These assumptions include the transportation modes, fuel types, energy intensities, and distances transported with each mode, as shown in Table S3. Crude oil is transported from the well to the refinery by ocean tanker, barge, pipeline, rail and truck, and refined MD products are transported and distributed by rail and truck.[27] GREET 2011 is also used to calculate the energy used during the crude oil extraction, recovery and refining processes. GREET 2011 energy assumptions are aggregated for each step and related to the primary energy sources of coal, natural gas and petroleum products. Other primary energy sources, such as wind or nuclear, are neglected due to their small contribution to overall water footprint. Figure S4 shows the indirect blue water consumption associated with each primary energy carrier based on Gleick, and the calculations shown in Section S2.[21] These values were used for the calculation of the indirect blue water consumption of the transportation steps for all pathways.

The transportation modes are fuelled by petroleum refinery products, including residual oil and diesel, and in the case of pipelines by natural gas and electricity. During the oil extraction, re-

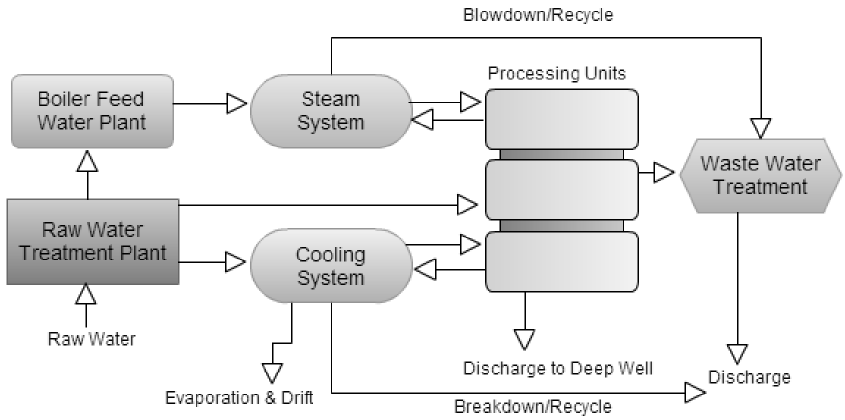

Figure S2: Water flow in a typical North American refinery, adapted from Wu et al.[26]

covery and refining steps, petroleum refinery products are used along with other energy sources. Therefore, estimation of the indirect water use associated with the production of all the fuels utilized during these transportation and processing steps requires iterative calculations. Direct water consumption from transportation has not been considered in this analysis due to its negligible contribution.[28]

The iterative procedure used in this analysis to estimate the direct and indirect water consumption from the processing and transportation steps is as follows:

1. The direct water consumption values given in Table S2 for the three PADDs are used as initial values in this analysis. The analysis is carried out for each PADD separately.

2. The direct water consumption values in Table S2 are allocated among a representative oil refinery product slate based on the energy contents of each fuel cut.[29] Lower heating values are taken from GREET 2011.[27]

3. Crude oil transportation uses diesel, residual oil, natural gas and electricity. Step 2 values for diesel and residual oil are used as inputs to determine the contribution of crude oil transportation, and the water intensity of natural gas is calculated as shown in Section S2.1. The water intensity of electricity is calculated for each PADD using data from Wu et al.[26] The results are allocated amongst the assumed product slate and added to the values calculated in step 2.

4. The values calculated in step 3 are used as petroleum refinery inputs to calculate the contribution from crude oil extraction and recovery. The water intensity for coal is taken from Gleick.[21] The results are allocated amongst the assumed product slate and added to the values calculated in step 3.

5. Using the water intensities calculated in step 4, along with the water intensities for natural gas and coal, the contribution from producing residual oil, ULS diesel, diesel, and conventional jet fuel is estimated. The results, specific to each fuel (and hence, already allocated), are then added to the values in step 4.

Table S3: Crude oil and finished fuel transportation assumptions for the conventional MD pathway from GREET 2011.[27]

	Mode[a]	Share[b]	Distance [km]
Crude oil transp.	Ocean tanker	57%	8179
	Barge	1%	805
	Pipeline	100%	1207
Residual oil transp.	Ocean tanker	24%	4828
	Barge	40%	547
	Pipeline	60%	644
Conventional MD Transp. & Dist.	Ocean tanker	16%	2333
	Barge	6%	837
	Pipeline	75%	644
	Rail	7%	1287
	Truck	100%	48

[a]Barge runs on residual oil; truck and rail run on diesel; and pipelines run on 20% diesel, 50% residual oil, 24% natural gas and 6% electricity. The energy intensities are 0.513, 1.49, 0.267 and 0.183 MJ/tonne-km, respectively.

[b]Mass-based share of a feedstock that relies on a certain transportation mode. The total can exceed 100% because feedstock may be moved from location to location by different transportation modes until it reaches its final destination.

Table S4: Indirect blue water consumption footprint of primary energy carriers.

Primary energy carrier	Indirect blue water consumption footprint [l_{water}/MJ_{energy}]
Coal	0.164
Natural gas	0.124
Petroleum	0.127
Diesel	0.153
Residual oil	0.166

6. The step 5 values, along with water intensities of natural gas and electricity, are used to calculate the contribution of transporting residual oil, ULS diesel, diesel, and conventional jet fuel. The calculated fuel-specific values are added to the step 5 results.
7. The water intensities calculated for residual oil and ULS diesel in step 6, along with those of coal and natural gas, are used to estimate the impacts of MD transportation. The calculated contributions for each PADD are then summed with the step 6 results.

Variability in the results for the conventional MD pathway is due to assumptions regarding the blue water consumption of crude oil recovery and extraction in the different PADDs from Wu et al.[26] This analysis expands on the blue water consumption footprint of conventional MD reported by Wu et al.[26] by including indirect blue water consumption from transportation, and material and energy inputs, and by allocating results amongst refinery fuel products.

S2.3 FT MD from coal and natural gas

The FT process converts any carbon-containing feedstock, such as natural gas, coal or biomass, to paraffinic hydrocarbons. The process involves steam reforming of natural gas, or gasification of a solid feedstock, into a mixture of carbon monoxide and hydrogren called synthesis gas, or syngas, which is then purified and converted to fuel via FT synthesis. Longer hydrocarbon chains are then cracked down to maximize the MD cut of the product slate. This analysis assumes that the energy requirements to produce FT MD are the same as those used in Stratton et al.[30] In addition, it is assumed that 70% of the product slate, by energy content, is MD, and that the plant is able to produce enough electricity for its own requirements.[30]

In this analysis two FT pathways are considered for fuel production: coal-to-liquids (CTL) and natural gas-to-liquids (GTL). For coal feedstock extraction, water is consumed during open pit and underground mining operations, and for washing to remove contaminants. For natural gas feedstock, water is consumed primarily during treatment to remove H_2S and CO_2. Underground mining of coal is more water intense than surface mining,[21] and natural gas production from shale is a more water intense process than conventional natural gas production.[31] The blue water consumption footprint for the extraction and treatment of these primary energy carriers are between 0.161 and 0.169 [l_{water}/MJ_{coal}] for coal, and 0.109 and 0.134 [l_{water}/MJ_{NG}] for natural gas.[21,23]

After the feedstock has been extracted it is transported to an FT refinery. The GREET 2011[27] assumptions for the energy intensity of coal and natural gas transportation to an FT facility are used to estimate the indirect water consumption of this step. These assumptions are shown in Table S5.

Table S5: Natural gas and coal feedstock transportation assumptions for the FT MD pathway from GREET 2011.[27]

Feedstock	Fuel	Energy intensity [J/MJ]
Natural gas	Coal	50
	Natural gas	921
	Petroleum	4
Coal	Coal	42
	Natural gas	187
	Petroleum	837

Once at the refinery, the first step in the FT process is steam reforming or gasification, during which the feedstock is partially oxidized into syngas. Purification of the syngas to remove impurities, such as sulfur, is crucial in order to prevent catalyst poisoning during the downstream FT synthesis. This is accomplished in a hydrotreatment process. Another important parameter in the FT synthesis is the CO-to-H_2 ratio that needs to be adjusted to minimize coking and maximize straight-chain hydrocarbon production. This ratio can be tuned through the water-gas shift (WGS) reaction, which requires fresh water input:

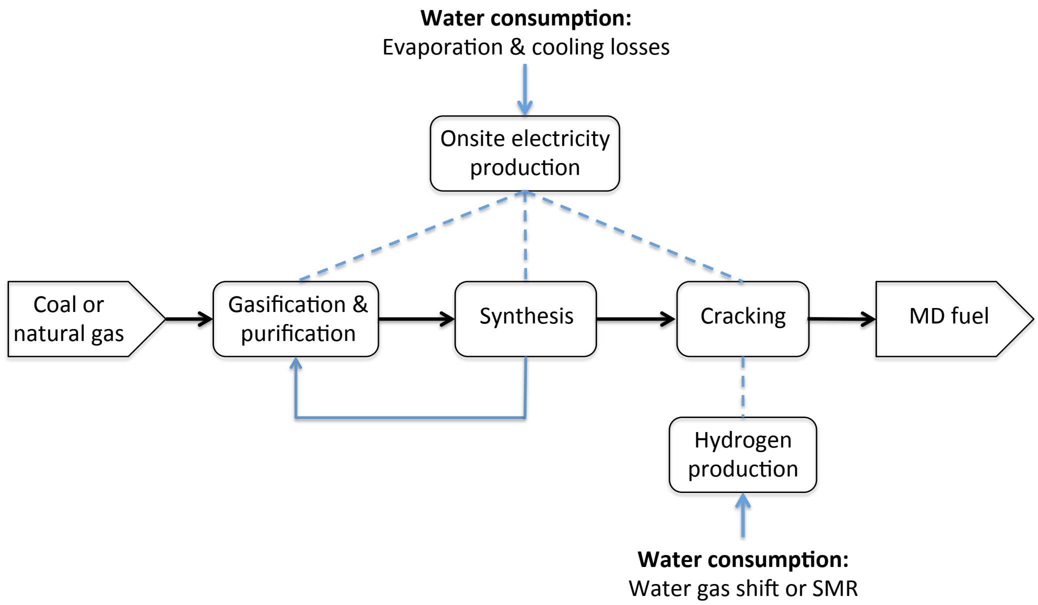

Figure S3: Simplified flow diagram of the FT process, water consumption highlighted.

$$H_2O + CO \rightarrow H_2 + CO_2$$

Following gasification and purification, FT synthesis takes place, which is a polymerization reaction of carbon monoxide in the presence of hydrogen and an iron- or cobalt-based catalyst.[30] The synthesis process is described by the following reaction:

$$\mathrm{mCO} + \frac{n+2m}{2}\mathrm{H}_2 \rightarrow \mathrm{C}_m\mathrm{H}_n + \mathrm{mH_2O}$$

Water produced as a by-product of FT synthesis can be treated for use within the FT process or other industrial processes. The gasification and synthesis processes both require electrical power, and most commercial facilities choose to produce electricity on-site. On-site electricity production requires additional fresh water for steam production and cooling.

In addition to the cooling system, water may be used directly in the FT process in a number of other ways, such as the WGS reaction. Steam methane reforming also requires fresh water, as it uses steam to convert methane into syngas. The reaction for steam methane reforming is as follows:

$$H_2O + CH_4 \rightarrow CO + 3H_2$$

A simplified process flow diagram of the FT fuel production process is shown in Figure S3, with water consumption highlighted. The transportation and distribution of FT MD is subject to the same assumptions as the other alternative MD pathways, for which the default GREET 2011 assumptions are shown in Table S6, including barge, truck and rail modes of transport.

Table S6: FT MD transportation assumptions from GREET 2011.[27]

	Mode[a]	Share[b]	Distance [km]
	Truck	63%	80.5
Alternative MD	Barge	8%	837
Transp. & Dist.	Rail	29%	1 287
	Truck (dist.)	100%	48

[a]Barge runs on residual oil, and truck and rail run on diesel. The energy intensities are 0.513 and 1.49 MJ/tonne-km, respectively.

[b]Mass-based share of a feedstock that relies on a certain transportation mode. The total can exceed 100% because feedstock may be moved from location to location by different transportation modes until it reaches its final destination.

In order to calculate the lifecycle blue water consumption of the CTL and GTL FT pathways, a range of process parameters are considered for each of the feedstock-to-fuel conversion processes. This is done in order to capture the effects of variability in technology implementation on the results. Table S7 shows the assumptions and associated references that define low, mid and high scenarios for each feedstock-to-fuel conversion process, including variability due to the feedstock extraction process, lower heating value (LHV) conversion efficiency, and direct process water use, from Bao et al.,[32] Matripragada,[33] and Stratton et al.[30]

Table S7: Variability of blue water consumption of FT MD pathways

Process	Case	Feedstock extraction	LHV conv. eff.	Process water consump. [l_{water}/l_{fuel}]	Fuel alloc.
CTL	Low	Surface mining[21]	53%[30]	7.5[33]	70%
	Mid	50% surface, 50% underground[21]	50%[30]	9.4[33]	70%
	High	Underground mining[21]	47%[30]	11.4[33]	70%
GTL	Low	Conventional gas[21]	65%[30]	0.0[32]	70%
	Mid	Conventional & shale gas[21]	63%[30]		70%
	High	Shale gas[23 21]	60%[30]		70%

S2.4 AF MD from sugarcane, corn, switchgrass

The AF MD pathway lifecycle includes biomass cultivation and transportation, feedstock-to-fuel conversion, and MD transportation and distribution. Three types of AF biomass feedstock are considered in this analysis. Sugary feedstocks include biomass in which mono- or disaccharide sugars, such as glucose and sucrose, are present in significant quantities; starchy feedstocks include biomass in which a polysaccharide, such as starch, is the main sugar component; and lignocellulosic feedstocks include biomass in which sugar is stored in complex polysaccharides, such as cellulose and hemicellulose. One representative feedstock from each class was selected for this analysis: sugarcane, corn and switchgrass, respectively. Water is consumed during cultivation of these feedstocks by evaporation and evapotranspiration. Estimation of blue water consumption associated with feedstock cultivation is discussed in detail in Section S1.3.

After the biomass has been harvested from the field it is transported to a bio-refinery. The AF feedstock transportation assumptions, shown in Table S8, are based on the default assumptions in GREET 2011.[27]

Table S8: AF feedstock transportation assumptions from GREET 2011.[27]

	Mode[a]	Share[b]	Distance [km]
Sugarcane	Truck	100%	19
Corn	Truck	100%	16
grain	Truck	100%	64
Switchgrass	Truck	100%	64

[a]Truck runs on diesel, with an energy intensity of 1.49 MJ/tonne-km.

[b]Mass-based share of a feedstock that relies on a certain transportation mode. The total can exceed 100% because feedstock may be moved from location to location by different transportation modes until it reaches its final destination.

Following cultivation and transportation to a processing facility, the feedstock undergoes pretreatment to extract the complex carbohydrate sugars, or polysaccharides, from the biomass. This typically involves mechanical size reduction and physical or chemical processing to extract the sugars from the structure of the feedstock.

In the case of sugarcane, the energy and water consumption intensity of sucrose extraction was estimated from a review of sugar-mill technologies.[34–37] Water consumption during sugarcane pretreatment is primarily due to losses during sugarcane washing, steam production and turbo-generator cooling during electricity co-production.[37] A simplified process flow diagram of the sugarcane pretreatment process is shown in Figure S4.

Starch is extracted from corn grain via milling pretreatment. The energy and water requirements of corn grain milling were estimated from a survey of the corn ethanol literature.[38–44] Water is consumed during evaporation from cooling and boiler feed water (BFW) make-up for cooking and liquefaction processes. Drying of distillers dried grains and solubles (DDGS) is also a major source of consumptive water use.[26] A simplified process flow diagram of the corn pretreatment process is shown in Figure S5.

In this analysis it is assumed that sugars are extracted from switchgrass using dilute acid pretreatment, and the associated energy and water consumption is estimated from the literature.[45–47] Water consumption during the pretreatment of switchgrass is due to evaporation from cooling processes, and from steam production and feedstock combustion during electricity co-production.[46] A simplified process flow diagram of the switchgrass pretreatment process is shown in Figure S6.

The steps following feedstock pretreatment are common to all of the AF pathways considered in this analysis. Saccharification is used to break down the polysaccharide molecules to monomeric C5 and C6 sugars. The sugar monomers are fed to a genetically engineered micro-organism that

Figure S4: Simplified process flow diagram of sugarcane milling pretreatment, water consumption highlighted.

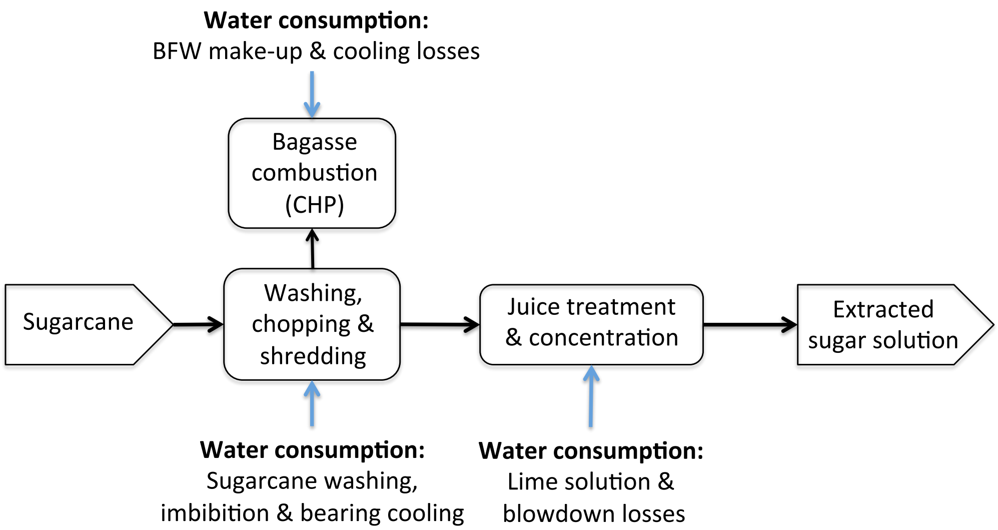

Figure S5: Simplified process flow diagram of corn grain milling pretreatment, water consumption highlighted.

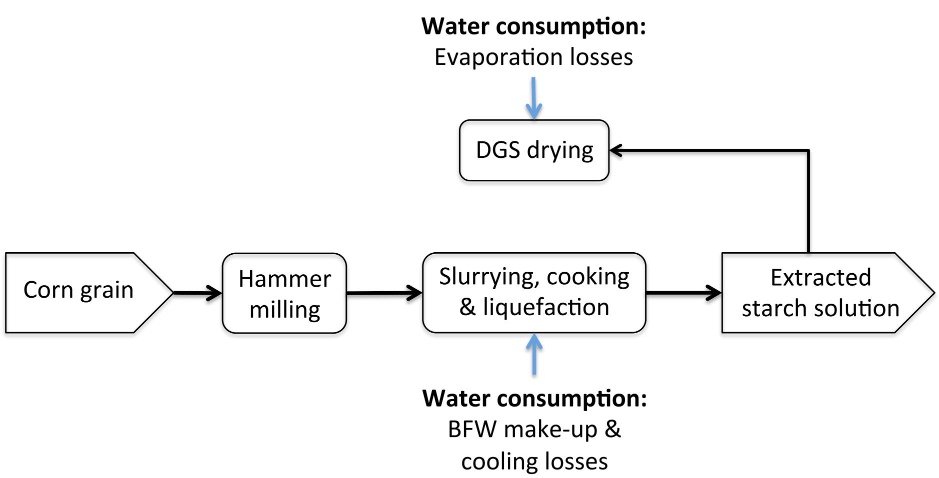

Figure S6: Simplified process flow diagram of switchgrass dilute acid pretreatment, water consumption highlighted.

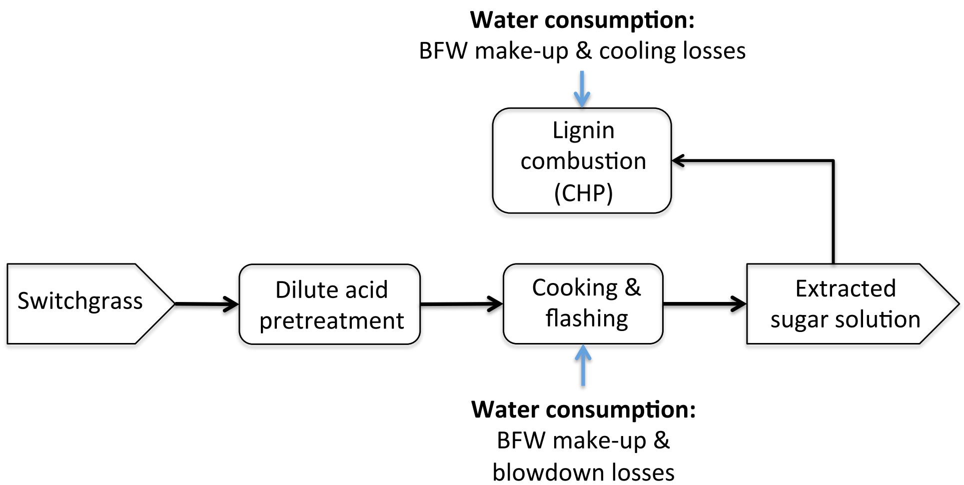

metabolizes the sugar to a platform molecule and CO_2. The energy and water consumption of saccharification and metabolism by the engineered micro-organism was estimated from ethanol plant data,[38–44] characteristic bioreactor values,[48] and consultation with researchers and industry.[49–52] During saccharification and metabolism, water is consumed primarily for cooling of the bioreactor.[37] It is assumed that the micro-organism employed metabolizes monomer sugars to alkanes, fatty acid, ethanol or isobutanol.

The platform molecules are then separated from the other products of metabolism and sent to post-processing for upgrading to a drop-in fuel product slate, including some MD fraction. Three technologies were considered for the separation and concentration of alkanes and fatty acids after metabolism; centrifugation,[53] hexane extraction,[30] and KOH steam lysing.[54] It is assumed that distillation is used to separate and concentrate ethanol and isobutanol following metabolism. Finally, the energy and water consumption requirements of upgrading platform molecules to a drop-in fuel slate were estimated through consultation with industry for ethanol and isobutanol platform molecules,[50,51] and by using the process parameters for hydroprocessing of esters and fatty acids, for alkane and fatty acid platform molecules.[54–56] The monomer sugar metabolism, platform molecule extraction, and post-processing steps are shown in Figure S7, and the data sources for the AF pathways are shown in Table S9. Transportation and distribution of AF MD fuel is subject to the same assumptions as the other alternative MD pathways, shown in Table S6.

The overall water footprints of the AF pathways are dependent upon the allocation methodology applied to the analysis. For all of the AF pathways, market allocation is used to allocated the water footprint between the co-products and the platform molecule produced.[57] The free-on-board prices for the co-products of the AF pathway, such as DDGS, wet distillers grain, corn gluten feed and corn gluten meal, are from the US Grain Council's weekly report.[58] The sugarcane and switchgrass AF pathways co-produce electricity, and the nationwide average electricity price is taken from EIA.[59] Prices for the platform molecules are from the Independent Chemical Information

Figure S7: Simplified process flow diagram of monomer sugar metabolism and upgrading to drop-in fuel, water consumption highlighted.

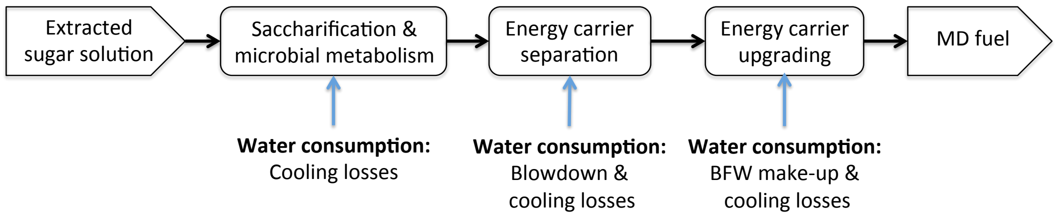

Table S9: Data sources for AF MD feedstock-to-fuel process parameters.

Process step	References
Sugarcane pretreatment	[34–37]
Corn pretreatment	[38–44]
Switchgrass pretreatment	[45–47]
Advanced fermentation	[49–52]
Platform molecule upgrading	[50,51,54–56]

Service (ISIC).[60] All prices are for August, 2012. Blue water consumption is allocated amongst the constituent fuel slate products using energy allocation. These allocation methods are consistent with previous lifecycle GHG emissions studies on alternative MD production pathways.[30] The parameters contributing to variability due to feedstock-to-fuel conversion process parameters are shown in Table S10.

Table S10: Feedstock-to-fuel process variability for blue water consumption of AF MD pathways.

Pathway	Scenario	Platform molecule	Power inputs [kWh/l_{MD}]	NG inputs [MJ/l_{MD}]	Make-up water [l_{water}/l_{MD}]	Feed-to-fuel [kg_{feed}/l_{MD}]	Co-prod. alloc.	Fuel alloc.
Sugarcane	Low	Alkanes	0	0	6.2	18.4	79%	81%
AF	Mid	Fatty acid	0	0	10.9	21.3	91%	81%
(50% moist.)	High	Ethanol	0	0	14.9	25.9	94%	78%
Corn	Low	Isobutanol	0.47	8.4	3.8	3.6	85%	100%
AF	Mid	Fatty acid	0.75	8.6	4.6	5.8	75%	81%
(15.5% moist.)	High	Ethanol	1.8	22.4	6.4	7.6	90%	78%
Switchgrass	Low	Alkanes	0	0	2.5	8.2	92%	81%
AF	Mid	Fatty acid	0.73	0	4.4	8.3	100%	81%
(0% moist.)	High	Ethanol	1.5	0	7.2	11.4	100%	78%

S2.5 HEFA MD and biodiesel from soybean, rapeseed and jatropha

The HEFA MD and biodiesel pathway lifecycles include biomass cultivation and transportation, vegetable oil extraction and transportation, vegetable oil to MD or biodiesel conversion, and MD fuel transportation and distribution.

Triglycerides or triacylglycerol (TAG), which consists of one glycerol and three fatty acid molecules, are the primary components of animal fats, vegetable and algal oils. These molecules can be hydrotreated into straight-chain alkanes, known as hydroprocessed esters and fatty acid (HEFA) fuels. Based on the type of feedstock, fatty acids can vary in size, and this will have a direct effect on the final product distribution. These fuels can then be isomerized to achieve better fuel properties, and catalytically cracked to maximize jet and naphtha production. Alternatively, TAGs can be transesterified into biodiesel.

This analysis considers soybean, rapeseed and jatropha for HEFA MD and biodiesel production. After the biomass has been harvested it is transported to an oil extraction mill by diesel-powered trucks. The biomass transportation assumptions, consistent with the default assumptions in GREET 2011,[27] are shown in Table S11.

Table S11: HEFA biomass transportation assumptions from GREET 2011.[27]

	Transportation step	Mode[a]	Share[b]	Distance [km]
Soybean	To stacks	Truck	100%	16
	Stacks to plant	Truck	100%	64
Rapeseed	To stacks	Truck	100%	16
	Stacks to plant	Truck	100%	64
Jatropha	To stacks	Truck	100%	16
	Stacks to plant	Truck	100%	64

[a]Trucks run on diesel, with an energy intensity of 3.18 and 2.48 MJ/tonne-km for oilseed and oil transportation, respectively.

[b]Mass-based share of a feedstock that relies on a certain transportation mode. The total can exceed 100% because feedstock may be moved from location to location by different transportation modes until it reaches its final destination.

Vegetable oil is extracted from the biomass by pressing the oilseeds and introducing an organic solvent, such as hexane.[56] In the case of soybean and rapeseed, the meal separated from the oil has a high protein content with commercial value as an animal feed, and market value allocation is used to allocate the water consumption to the meal co-product of oil extraction.

Jatropha has a structure that is quite different than the other oil seeds, resulting in co-products other than just the meal. The jatropha fruit is essentially a capsule containing a husk and two or three seeds. Each of the seeds has a shell and an oil-containing kernel. After the oil has been extracted from the kernel, the meal is leftover. Most varieties of jatropha fruit are toxic to humans and therefore this analysis assumes combustion of all the co-products (husks, shells and meal) for electricity generation.[30] Energy allocation is used to allocate water consumption to the electricity co-product of jatropha oil extraction.

The direct fresh water consumption associated with oil extraction from oil crops is due to BFW steam generation and cooling water make-up. The indirect fresh water consumption comes from the production of the material and energy inputs used in the extraction process, such as natural gas, electricity and hexane. The extracted oil is then transported to the HEFA plant to be converted into fuel via the HEFA process. The assumptions for transportation of oil to the HEFA facility, are shown in Table S12.

Table S12: HEFA oil feedstock transportation assumptions from GREET 2011.[27]

	Mode[a]	Share[b]	Distance [km]
Soybean oil	Truck	40%	129
Jatropha oil	Barge	40%	837
	Rail	20%	1127
Rapeseed oil	Truck	67%	129
	Rail	33%	1127

[a]Barges use residual oil, and trucks and rail run on diesel fuel. The energy intensities are 1.49 and 0.513 MJ/tonne-km, respectively.

[b]Mass-based share of a feedstock that relies on a certain transportation mode. The total can exceed 100% because feedstock may be moved from location to location by different transportation modes until it reaches its final destination.

Figure S8 shows a simplified process flow diagram of the HEFA MD process considered in this study. Vegetable oil is taken from feed storage and fed into a hydrodeoxygenation reactor where the olefinic double bonds of the TAGs are saturated in the presence of hydrogen, and the oxygen content is removed in the form of water and CO_2. During this reaction glycerol is separated from the rest of the TAG structure in the form of propane. The hydrodeoxygenation reaction generates water, which is treated for reuse in the boiler or cooling water system, rather than discharged to the sewer. The hydrogen required for hydrodeoxygenation is obtained from steam reforming (SMR) of natural gas. Water is used as a reactant in the SMR reactor. This is an endothermic reaction, and the heat required is supplied by high-pressure steam generated from BFW by burning natural gas.

The effluent from the hydrodeoxygenation reactor is then cooled down as steam is generated, and sent to an isomerization unit where cracking also takes place. The isomerized product is later cooled with cooling water and phase-separated into gases and liquids. The liquids are separated into different fuel products in a distillation unit, where steam is used for heating the boiler section. Gases are sent to a gas-processing unit where hydrogen and CO_2 are separated in a pressure swing absorption (PSA) unit. The gas-processing unit uses cooling water to facilitate the separation of methane, ethane and propane from water and other impurities to produce a dry gas suitable for use as a fuel. These gases are further purified, and can be used as process fuel in the process, or in the SMR unit, which is assumed to use natural gas in this analysis. Unreacted hydrogen is recycled back to the hydrodeoxygenation reactor.

Figure S8: Simplified process flow diagram of HEFA MD process, water consumption highlighted.

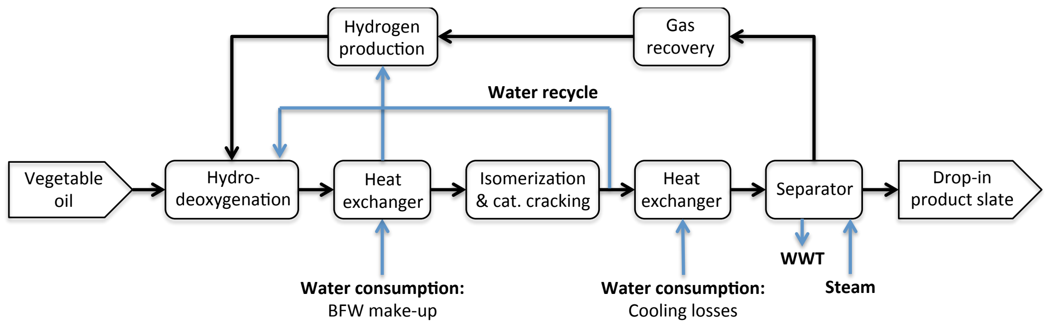

The liquid products from this process include liquefied petroleum gas (LPG), naphtha, jet fuel and diesel fuel. 91.5% of this product slate is composed of middle distillate fuels.[61–64] The design used in this analysis integrates the BFW with the process, such that make-up water demand may be reduced by generating steam instead of using cooling water. Hence, the direct fresh water consumed during the HEFA process is primarily due to the losses in the BFW that is used for steam generation and as cooling water, as shown in Figure S8. 89% of direct fresh water consumption is for boiler feed water makeup due to steam generation and cooling losses.[55] The indirect water consumed by the HEFA process is primarily due to the electricity and natural gas requirements of the process. Electricity is used to power pumps, compressors and other electrical controls around the refinery, and natural gas is used as a process fuel that is burned to supply heat in various units around the refinery, such as in the boiler of the SMR unit. Energy based allocation is used to allocate the fresh water consumption within the HEFA process amongst the fuel co-products. Table S13 summarizes the consumptive fresh water associated with the HEFA process.

Table S13: Blue water consumption of the HEFA MD feedstock-to-fuel process from Pearlson et al.[55]

	Direct blue water consumption [l_{water}/l_{oil}]
BFW make-up	0.8
SMR	0.2
Produced water	-0.1
Total	0.9

Alternatively TAGs can be transesterified to biodiesel, during which TAGs react with an alcohol in the presence of a catalyst. The glycerol backbone separates from the TAG leaving three fatty acid molecules, which form fatty acid alkyl esters (or biodiesel) by including alcohol into their structures. When methanol is used in this process, fatty acid methyl esters (FAME) are formed. In this analysis, default values and assumptions from GREET 2011 are employed for the processing steps.[27] The HEFA MD and biodiesel produced by these processes is then transported and distributed to its final destination, subject to the same assumptions as the other alternative MD pathways shown in Table S6.

Variability in the lifecycle results for the HEFA MD and biodiesel pathways is due to the choice of feedstock; biomass growth, oil extraction and oil yield assumptions; whether biomass is rainfed or irrigated, and the assumed location of biomass and fuel production. The parameters contributing to this variability due to process inputs and yields are shown in Table S14.

Table S14: Process variability of blue water consumption of HEFA MD and biodiesel pathways. Biomass growth input, oil extraction input and oil yield data from Stratton et al.[30]

Pathway	Scenario	Biomass growth [MJ/kg$_{feed}$]	Oil extract. [MJ/kg$_{oil}$]	Oil yield [kg$_{feed}$/kg$_{oil}$]	Co-prod. alloc.	MD alloc.	Biodiesel alloc.
	Low	Direct = 0.65 Indirect = 0.30	Direct = 8.22 Indirect = 0.17	4.7	47%	92%	90%
Soybean HEFA	Mid	Direct = 0.76 Indirect = 0.39	Direct = 8.22 Indirect = 0.17	4.7	47%	92%	90%
	High	Direct = 1.11 Indirect = 0.39	Direct = 8.22 Indirect = 0.17	4.7	47%	92%	90%
	Low	Direct = 0.28 Indirect = 0.91	Direct = 2.75 Indirect = 0.30	2.3	77%	92%	90%
Rapeseed HEFA	Mid	Direct = 0.42 Indirect = 1.25	Direct = 2.84 Indirect = 0.27	2.4	76%	92%	90%
	High	Direct = 0.91 Indirect = 1.71	Direct = 3.02 Indirect = 0.32	2.5	74%	92%	90%
	Low	Direct = 1.23 Indirect = 1.98	Direct = 2.45 Indirect = 0.22	3.0	70%	92%	90%
Jatropha	Mid	Direct = 1.39 Indirect = 2.14	Direct = 2.51 Indirect = 0.21	3.0	70%	92%	90%
	High	Direct = 1.56 Indirect = 2.21	Direct = 2.58 Indirect = 0.22	3.0	70%	92%	90%

S3 Tabular results

Table S15: Blue water consumption by lifecycle step for conventional MD, FT and rainfed MD production pathways under mid assumptions [l_{water}/l_{MD}]

Pathway	Feedstock growth/extraction	Feedstock transp.	Veg. oil extraction	Veg. oil transp.	Feedstock-to-fuel conversion	MD fuel transp.	Total	Assumed location of biomass cultivation
Conv. MD	3.37	0.00	-	-	1.72	0.03	5.12	-
Coal FT MD	10.93	0.00	-	-	6.58	0.03	17.54	-
NG FT MD	6.56	0.00	-	-	0.00	0.03	6.59	-
Sugarcane AF MD	-	0.11	-	-	10.23	0.03	10.37	Palm Beach, FL
Corn AF MD	-	0.12	-	-	7.43	0.03	7.58	La Salle, IL
Switchgrass AF MD	-	0.10	-	-	6.87	0.03	7.00	Robertson, TN
Soybean HEFA MD	-	0.06	0.55	0.04	1.45	0.03	2.14	Cass, ND
Rapeseed HEFA MD	-	0.05	0.38	0.03	1.50	0.02	1.98	Latah, ID
Jatropha HEFA MD	-	0.06	0.50	0.04	1.55	0.02	2.17	Palm Beach, FL
Soybean biodiesel	-	0.06	0.52	0.04	1.38	0.04	2.04	Cass, ND
Rapeseed biodiesel	-	0.05	0.36	0.03	1.41	0.04	1.92	Latah, ID
Jatropha biodiesel	-	0.06	0.48	0.04	1.44	0.04	2.05	Palm Beach, FL

Table S16: Blue water consumption by lifecycle step for irrigated MD production pathways under mid assumptions [l_{water}/l_{MD}]

Pathway	Feedstock growth/extraction	Feedstock transp.	Veg. oil extraction	Veg. oil transp.	Feedstock-to-fuel conversion	MD fuel transp.	Total	Assumed location of biomass cultivation
Sugarcane AF MD	482.57	0.11	-	-	10.23	0.03	492.94	Palm Beach, FL
Corn AF MD	302.96	0.12	-	-	7.43	0.03	310.54	La Salle, IL
Switchgrass AF MD	400.49	0.10	-	-	6.87	0.03	407.49	Robertson, TN
Soybean HEFA MD	1405.25	0.06	0.55	0.04	1.45	0.03	1407.38	Cass, ND
Rapeseed HEFA MD	1457.4	0.05	0.38	0.03	1.50	0.02	1459.38	Latah, ID
Jatropha HEFA MD	279.31	0.06	0.50	0.04	1.55	0.02	278.6	Palm Beach, FL
Soybean biodiesel	1333.75	0.06	0.52	0.04	1.38	0.04	1335.79	Cass, ND
Rapeseed biodiesel	1383.76	0.05	0.36	0.03	1.41	0.04	1413.92	Latah, ID
Jatropha biodiesel	265.22	0.06	0.48	0.04	1.44	0.04	267.27	Palm Beach, FL

Table S17: Rainfed blue and green water comsumption footprint tabular data from Figure 1. [l_{water}/l_{MD}]

	Blue			Green		
	Low	Mid	High	Low	Mid	High
Jatropha biodiesel	1.64	2.05	2.25	19.57	2054.71	18682.74
Rapeseed biodiesel	1.73	1.92	2.07	7.24	1790.54	9598.86
Soybean biodiesel (King & Webber)	0.12	0.33	0.53	–	–	–
Soybean biodiesel	1.88	2.04	2.51	3.72	1968.14	14783.24
Jatropha HEFA MD	1.66	2.17	2.41	20.16	2164.03	19219.52
Rapeseed HEFA MD	1.73	1.98	2.19	5.43	1885.80	9874.64
Soybean HEFA MD	1.95	2.14	2.71	8.56	2072.88	15208.16
Switchgrass EtOH (Wu et al.)	3.06	9.42	15.78	–	–	–
Corn stover E85 (King & Webber)	5.41	5.53	5.64	–	–	–
Switchgrass AF MD	6.05	7.00	18.09	19.88	3005.17	5051.28
Corn grain and stover EtOH (Scown et al.)	7.59	11.21	17.31	–	–	–
Corn grain E85 (King & Webber)	3.39	5.64	7.90	–	–	–
Corn grain AF MD	2.10	7.58	18.34	1.10	2485.12	13415.83
Sugarcane AF MD	7.73	10.37	16.08	32.00	2327.97	4408.67
Coal FT diesel (King & Webber)	5.11	10.36	15.60	–	–	–
Coal FT MD	15.41	17.54	20.07	–	–	–
NG FT diesel (King & Webber)	3.23	7.26	11.30	–	–	–
NG FT MD	5.62	6.59	7.47	–	–	–
Gasoline from conv. crude (Wu et al.)	3.60	5.29	6.99	–	–	–
Gasoline from conv. crude (Scown et al.)	4.86	9.26	12.12	–	–	–
Diesel from conv. crude (King & Webber)	1.41	2.12	2.82	–	–	–
MD from conv. crude	4.11	5.12	7.43	–	–	–

Table S18: Irrigated blue and green water comsumption footprint tabular data from Figure 1. [l_{water}/l_{MD}]

	Blue			Green		
	Low	Mid	High	Low	Mid	High
Jatropha biodiesel	2.94	267.27	15758.54	21.60	2054.71	18682.74
Rapeseed biodiesel	2.61	1413.92	21936.75	6.94	1790.54	9598.86
Soybean biodiesel (King & Webber)	15.85	324.93	634.02	–	–	–
Soybean biodiesel (Chiu & Wu)	0.10	321.74	11417.03	91.33	5771.03	9892.70
Soybean biodiesel	2.90	1335.79	14448.11	10.25	1968.14	14783.24
Jatropha HEFA MD	3.10	280.77	16554.38	20.17	2165.30	19230.79
Rapeseed HEFA MD	2.71	1459.38	22640.05	5.43	1886.91	9880.43
Soybean HEFA MD	3.10	1407.38	15215.75	8.56	2074.10	15217.07
Miscanthus EtOH (Scown et al.)	4.89	11.29	228.70	–	–	–
Corn stover E85 (King & Webber)	60.88	549.05	1037.21	–	–	–
Wheat straw EtOH (Chiu & Wu)	8.05	223.78	5819.95	1865.25	3299.94	5166.57
Corn stover EtOH (Chiu & Wu)	8.05	212.51	6272.34	288.87	1507.60	2869.40
Switchgrass AF MD	6.23	407.49	5801.00	19.89	3006.93	5054.24
Corn grain EtOH (Wu et al.)	16.10	268.86	521.62	–	–	–
Corn grain and stover EtOH (Scown et al.)	7.59	119.63	1582.69	–	–	–
Corn grain E85 (King & Webber)	29.31	713.65	1397.98	–	–	–
Corn grain EtOH (Chiu & Wu)	-945.04	49.91	2912.39	288.87	1077.06	1865.25
Corn grain AF MD	3.60	310.54	17286.00	1.10	2486.83	13423.69
Sugarcane AF MD	7.78	492.94	5660.43	32.02	2329.34	4411.26
MD from conv. crude	4.11	5.12	7.43	–	–	–

S4 Marginal resource requirement curves

This page left blank intentionally.

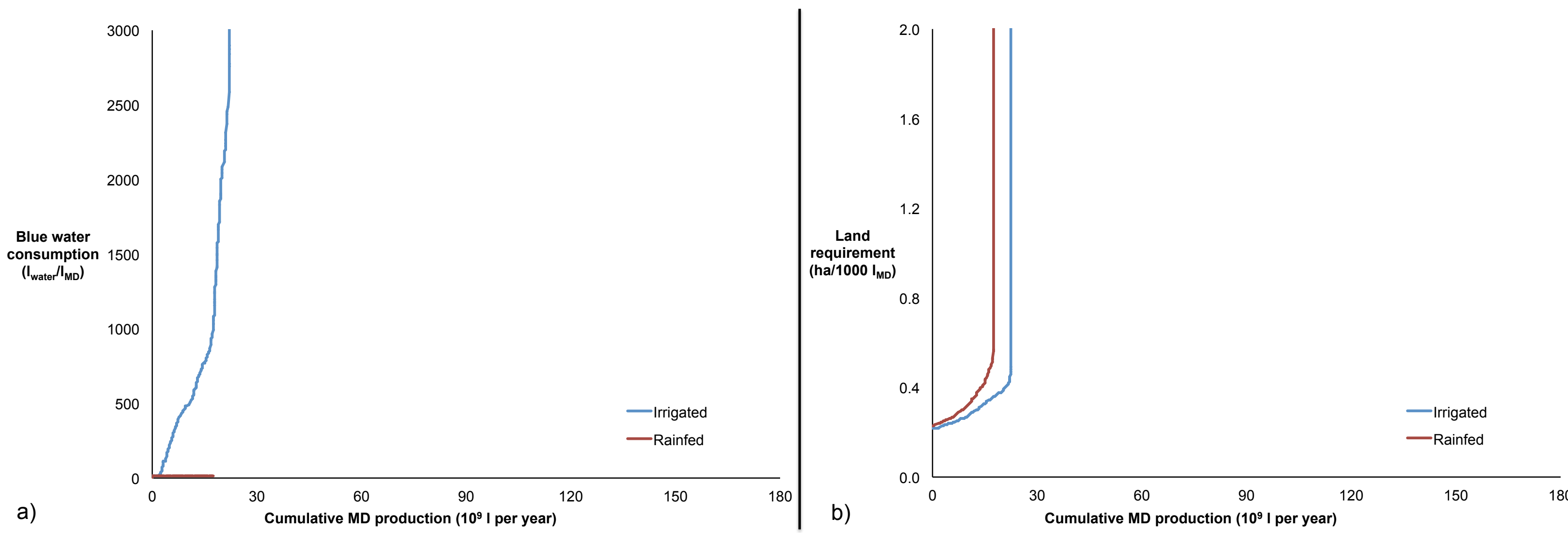

Figure S9: a) Marginal blue water consumption of rainfed and irrigated sugarcane AF MD production, counties ranked to minimize water requirements. b) Land requirements of rainfed and irrigated sugarcane AF MD production, counties ranked to minimize land requirements.

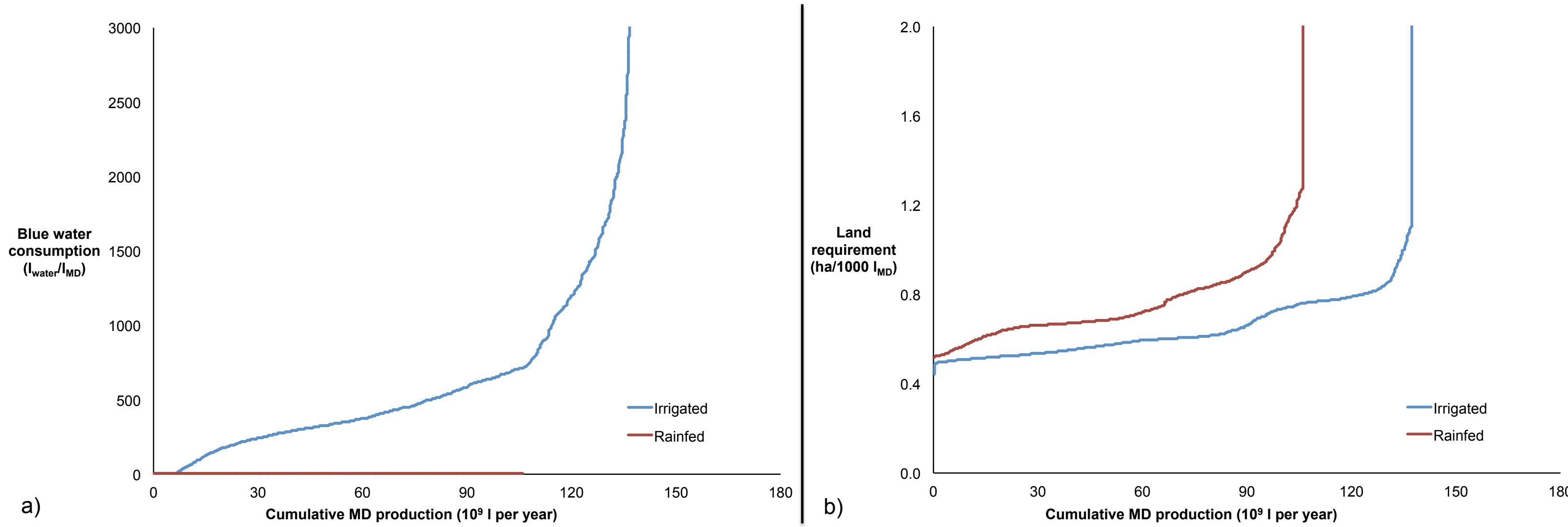

Figure S10: a) Marginal blue water consumption of rainfed and irrigated corn AF MD production, counties ranked to minimize water requirements. b) Land requirements of rainfed and irrigated corn AF MD production, counties ranked to minimize land requirements.

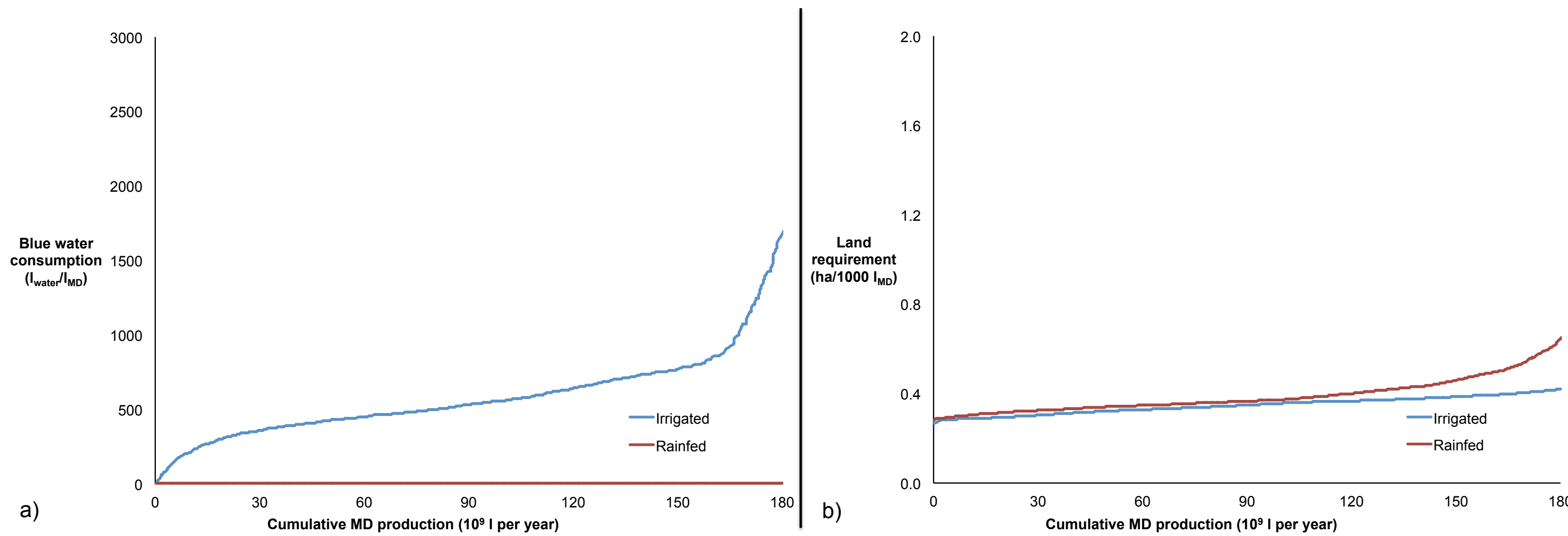

Figure S11: a) Marginal blue water consumption of rainfed and irrigated switchgrass AF MD production, counties ranked to minimize water requirements. b) Land requirements of rainfed and irrigated switchgrass AF MD production, counties ranked to minimize land requirements.

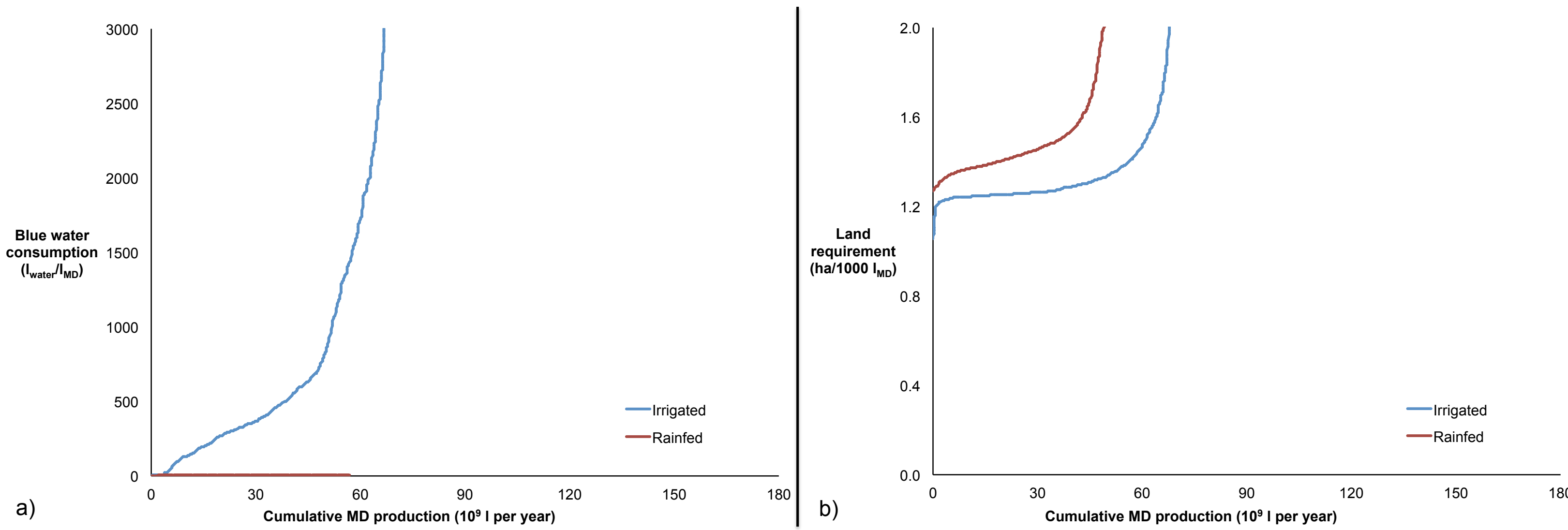

Figure S12: a) Marginal blue water consumption of rainfed and irrigated soybean HEFA MD production, counties ranked to minimize water requirements. b) Land requirements of rainfed and irrigated soybean HEFA MD production, counties ranked to minimize land requirements.

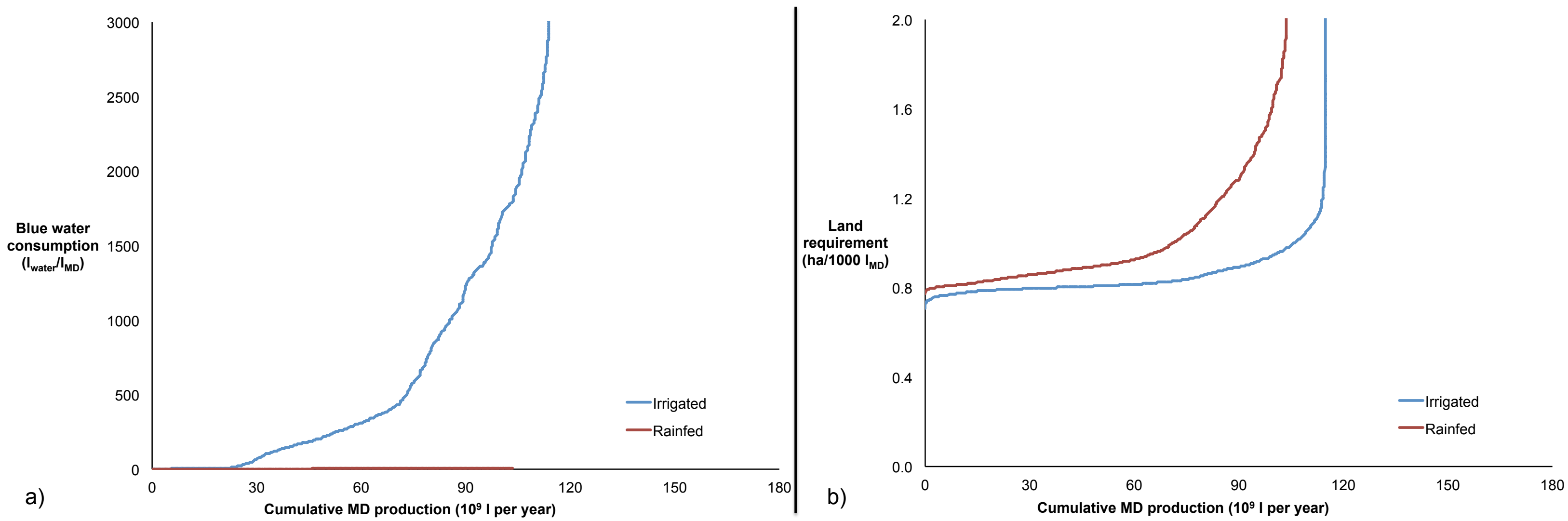

Figure S13: a) Marginal blue water consumption of rainfed and irrigated rapeseed HEFA MD production, counties ranked to minimize water requirements. b) Land requirements of rainfed and irrigated rapeseed HEFA MD production, counties ranked to minimize land requirements.

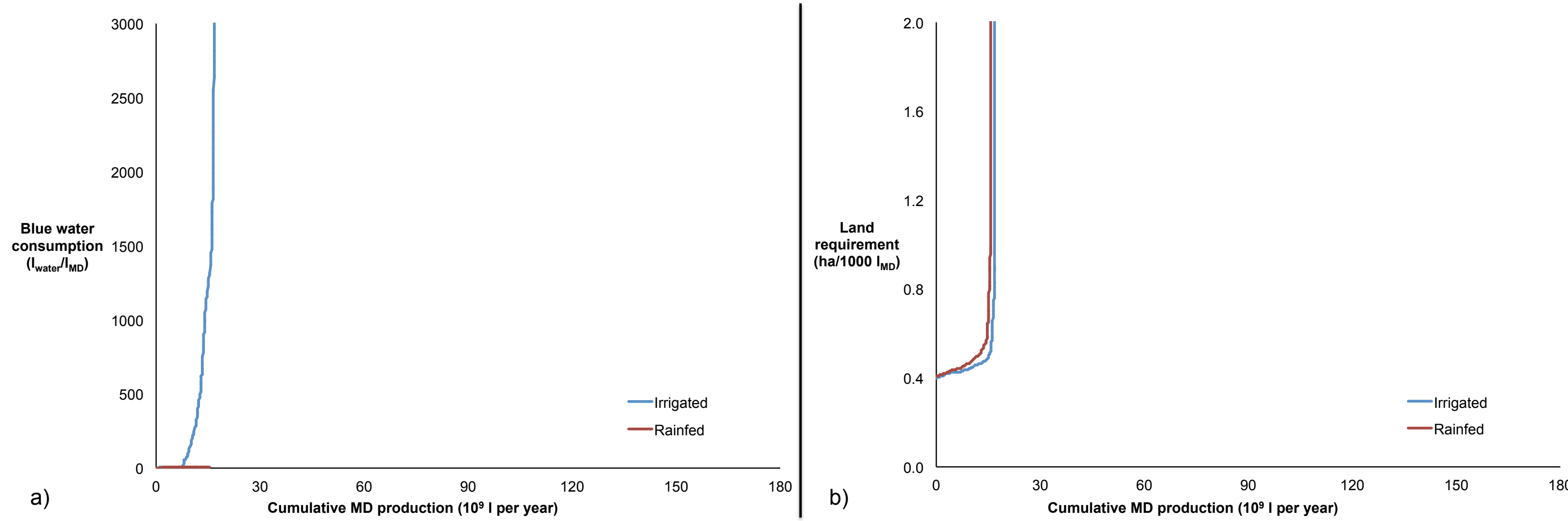

Figure S14: a) Marginal blue water consumption of rainfed and irrigated jatropha HEFA MD production, counties ranked to minimize water requirements. b) Land requirements of rainfed and irrigated jatropha HEFA MD production, counties ranked to minimize land requirements.

S5 Feedstock-to-fuel pathway maps

This page left blank intentionally.

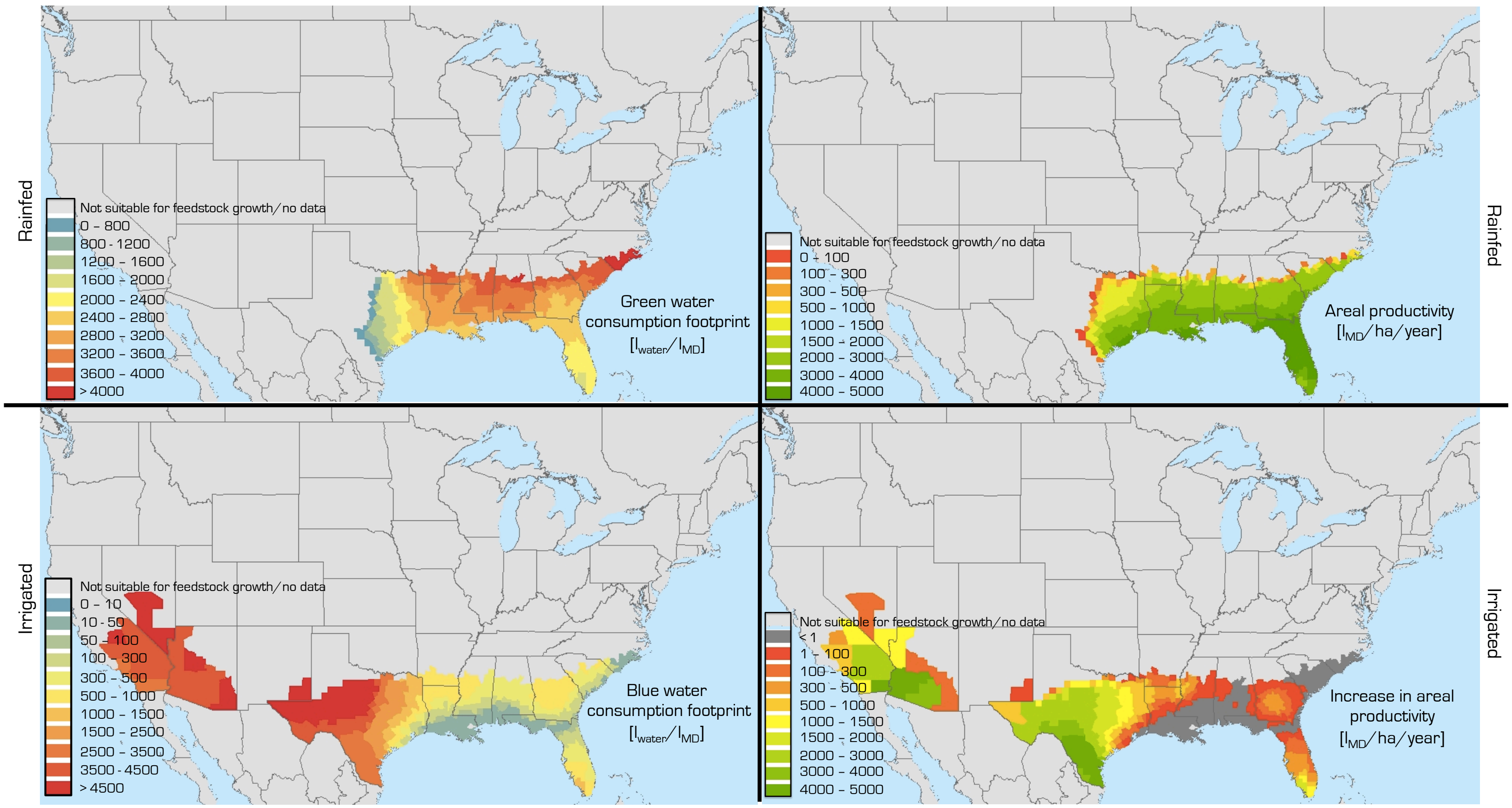

Figure S15: Lifecycle water consumption footprint and areal productivity of rainfed and irrigated sugarcane AF MD production.

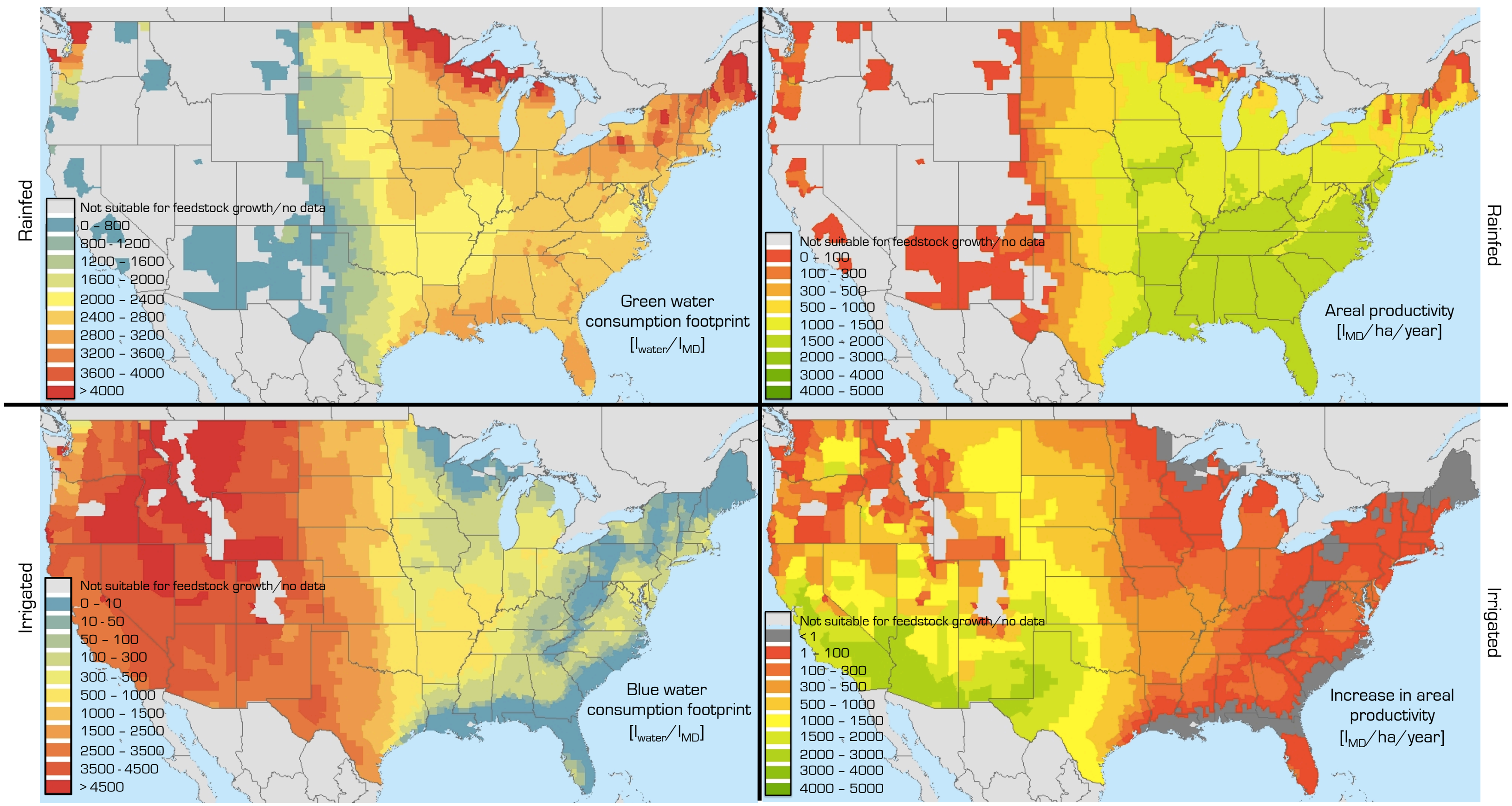

Figure S16: Lifecycle water consumption footprint and areal productivity of rainfed and irrigated corn AF MD production.

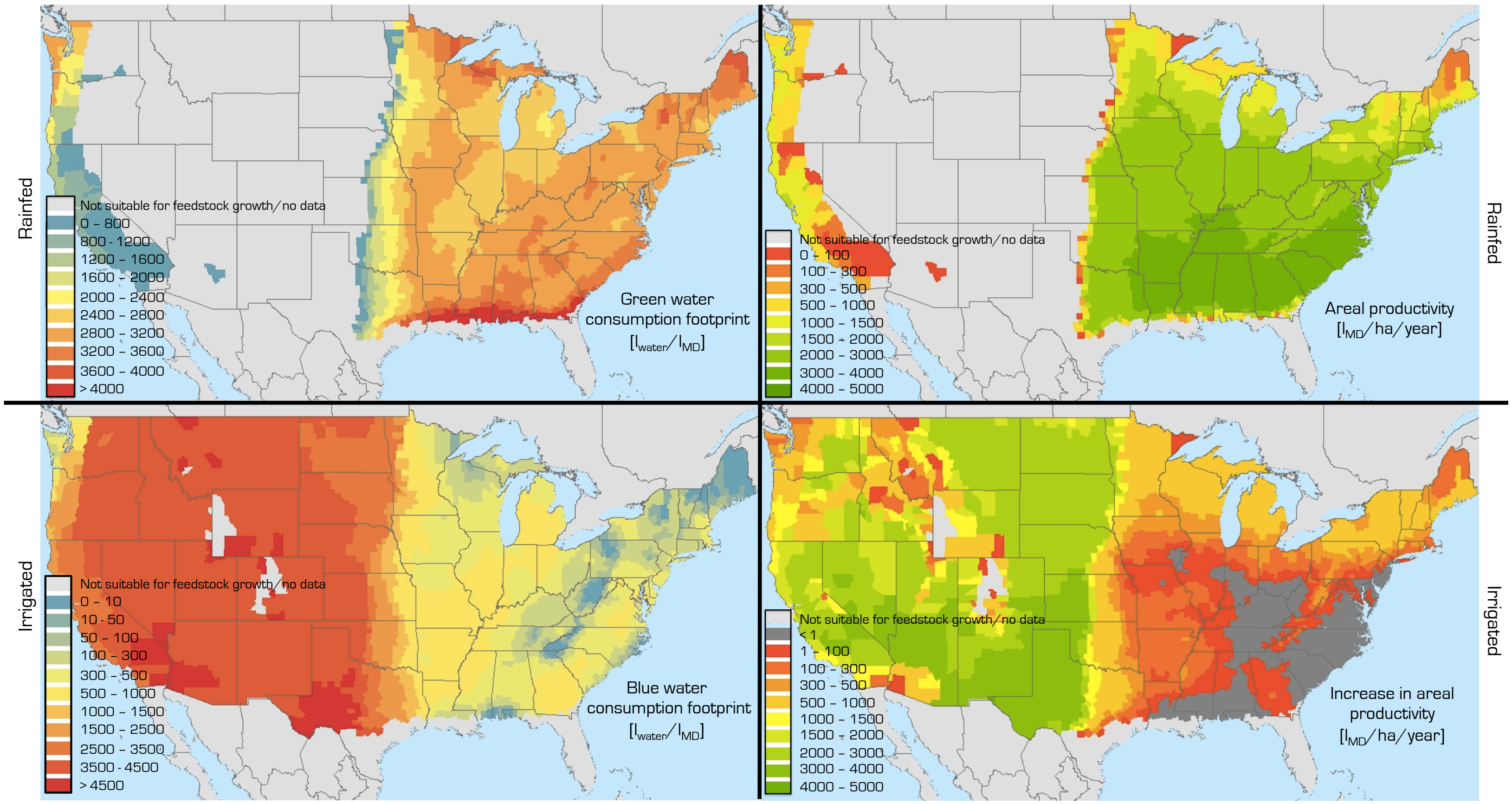

Figure S17: Lifecycle water consumption footprint and areal productivity of rainfed and irrigated switchgrass AF MD production.

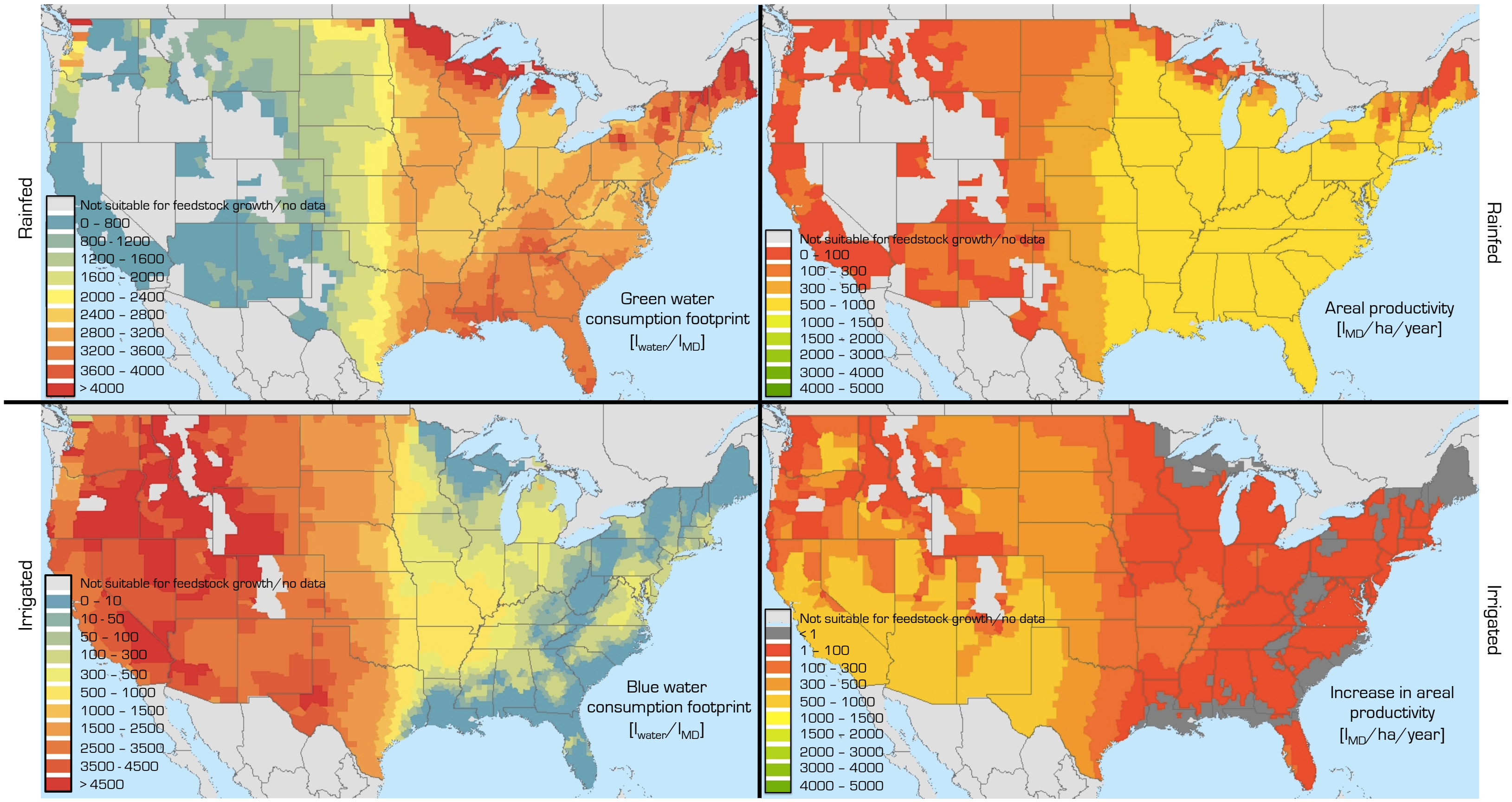

Figure S18: Lifecycle water consumption footprint and areal productivity of rainfed and irrigated soybean HEFA MD production.

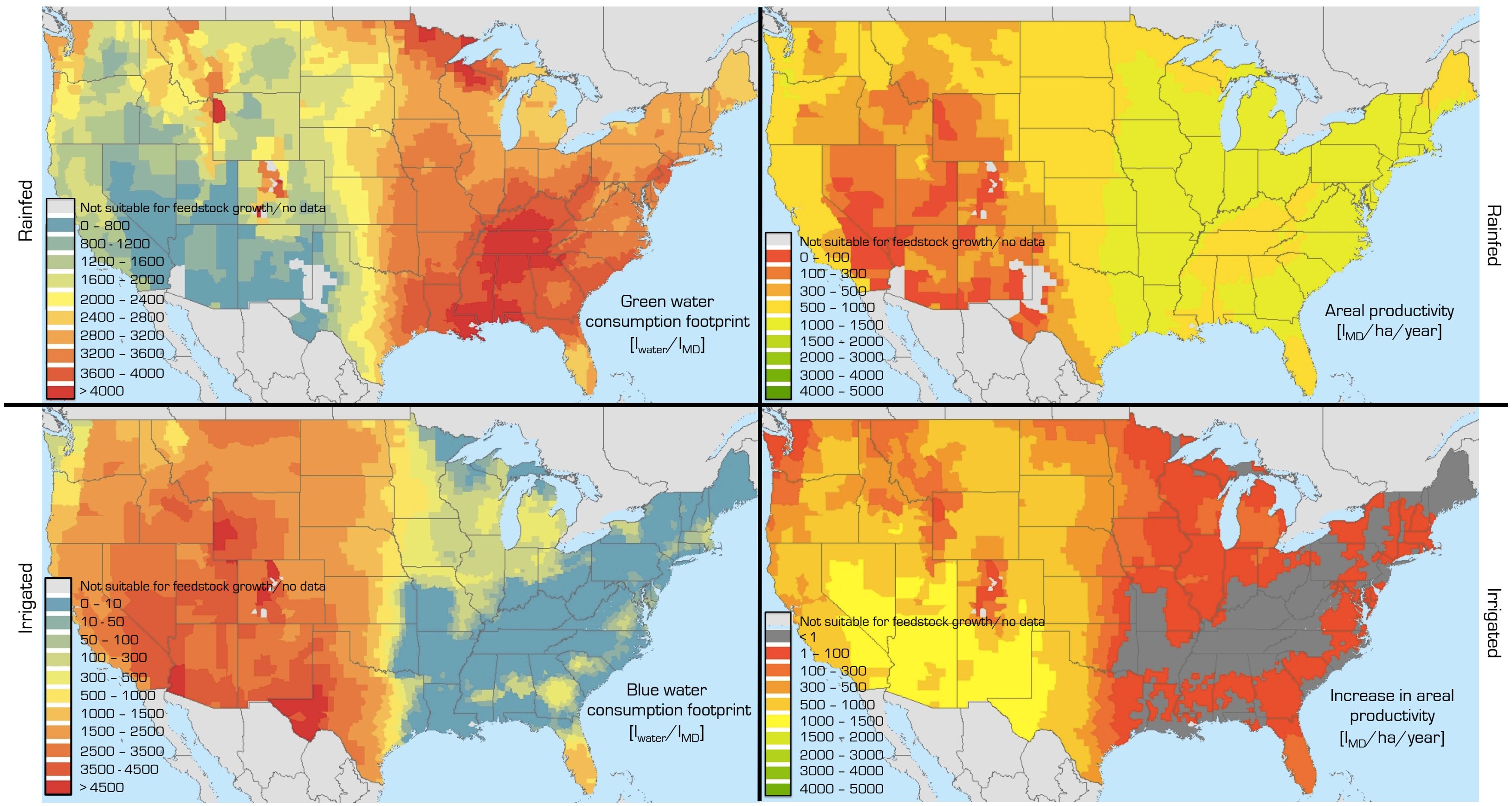

Figure S19: Lifecycle water consumption footprint and areal productivity of rainfed and irrigated rapeseed HEFA MD production.

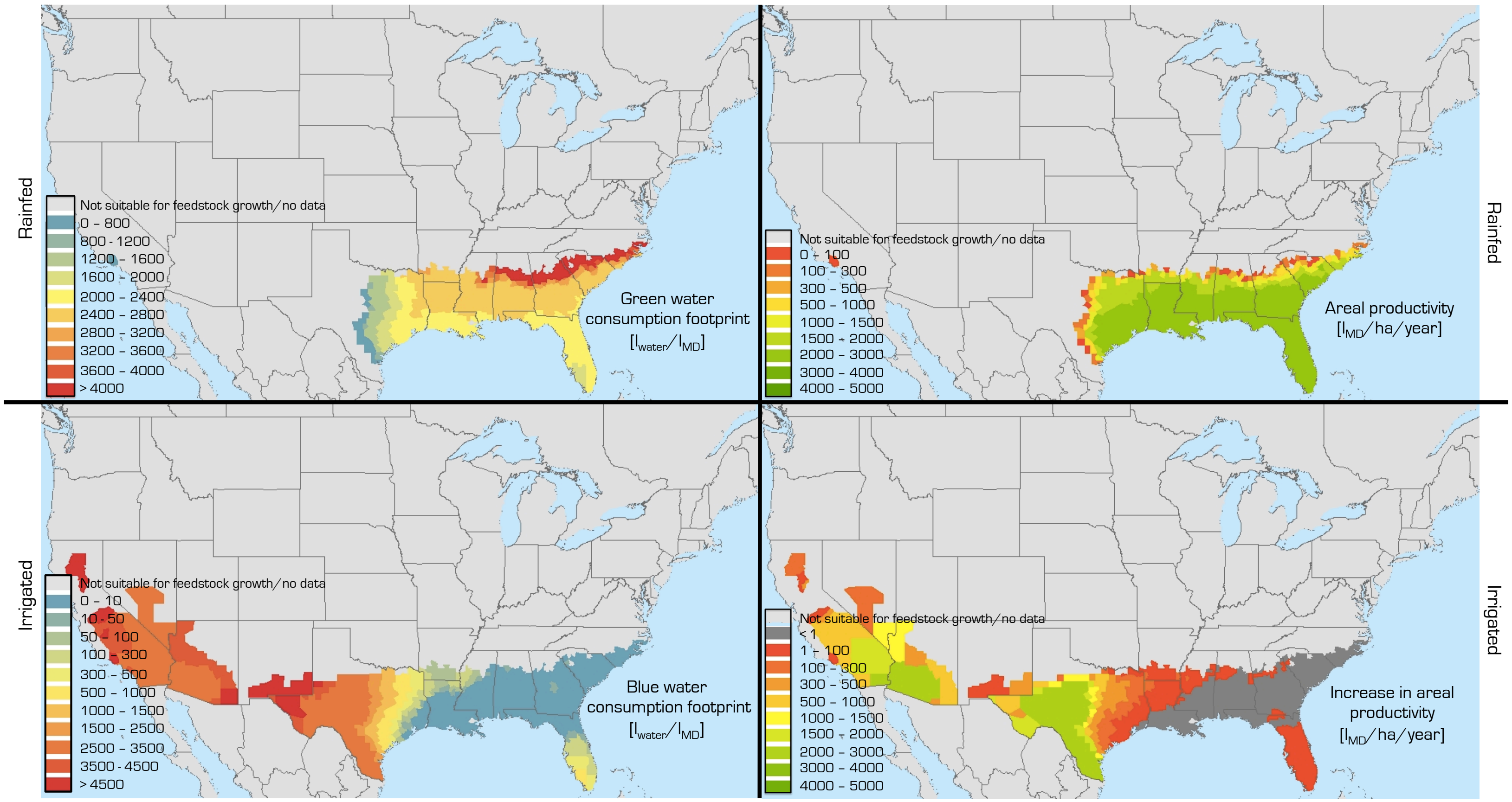

Figure S20: Lifecycle water consumption footprint and areal productivity of rainfed and irrigated jatropha HEFA MD production.

S6 Areal productivity benefit maps

This page left blank intentionally.

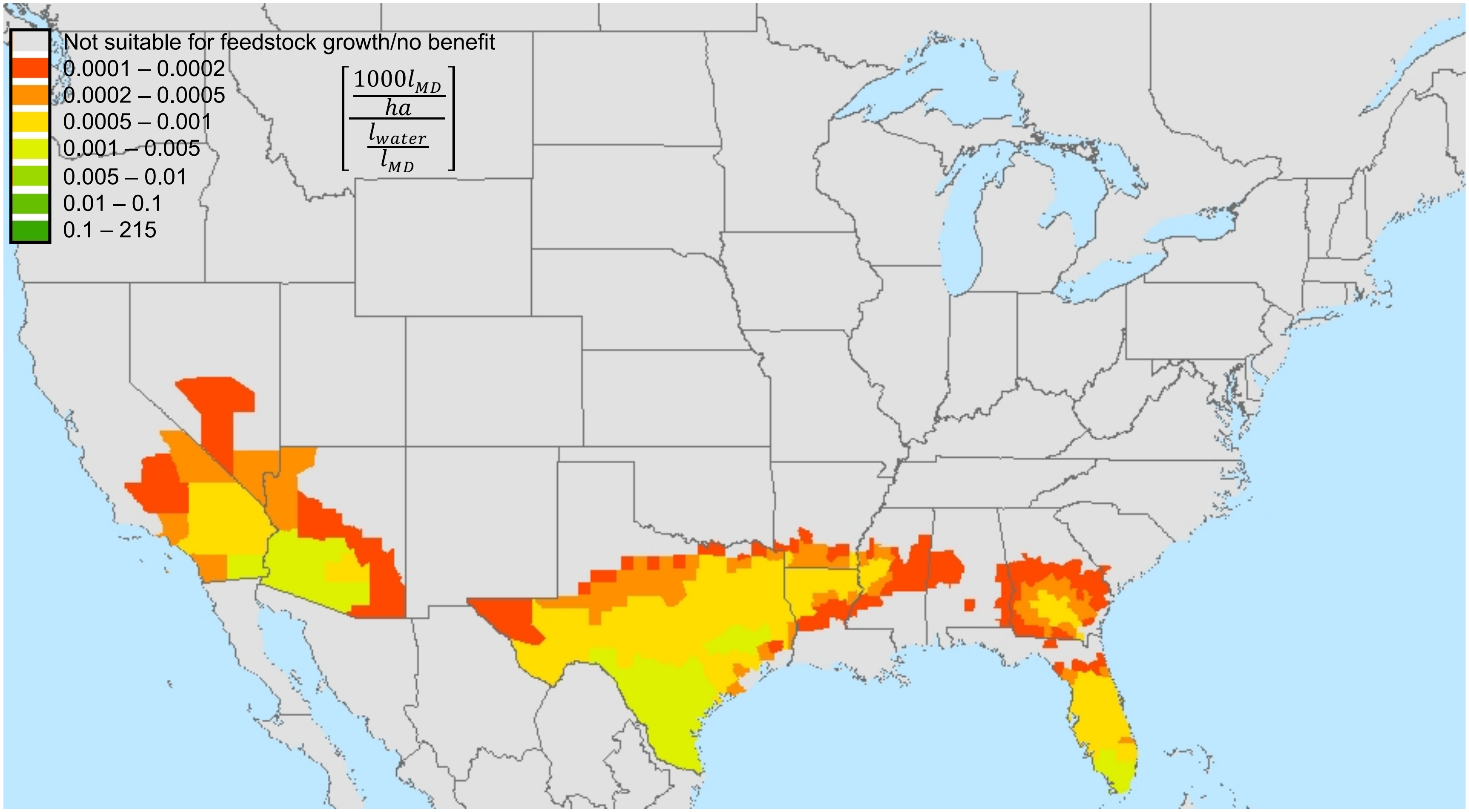

Figure S21: Areal productivity benefit of irrigation for sugarcane AF MD production. $[\frac{\frac{1000 l_{MD}}{ha}}{\frac{l_{water}}{l_{MD}}}]$

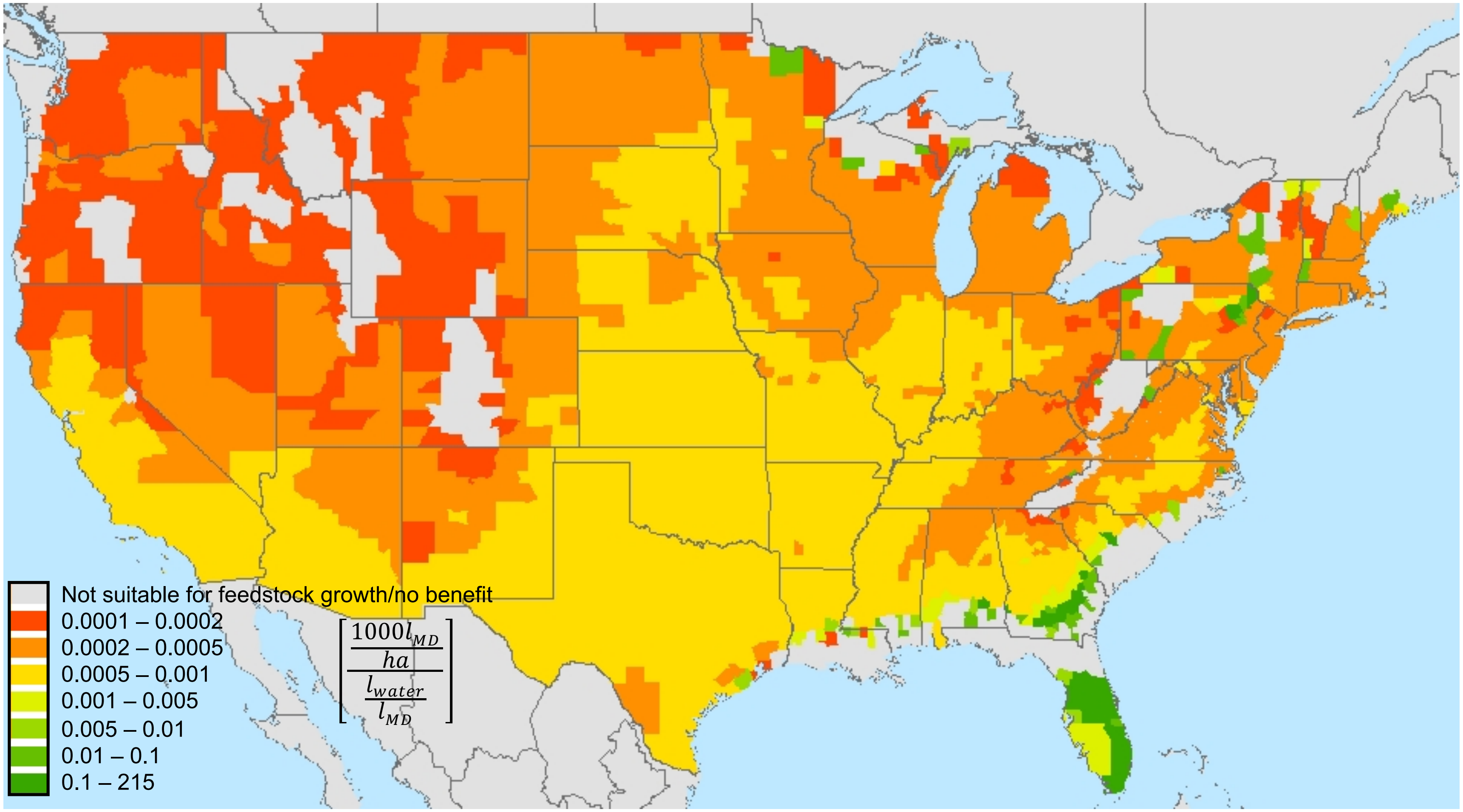

Figure S22: Areal productivity benefit of irrigation for corn AF MD production. $[\frac{\frac{1000 l_{MD}}{ha}}{\frac{l_{water}}{l_{MD}}}]$

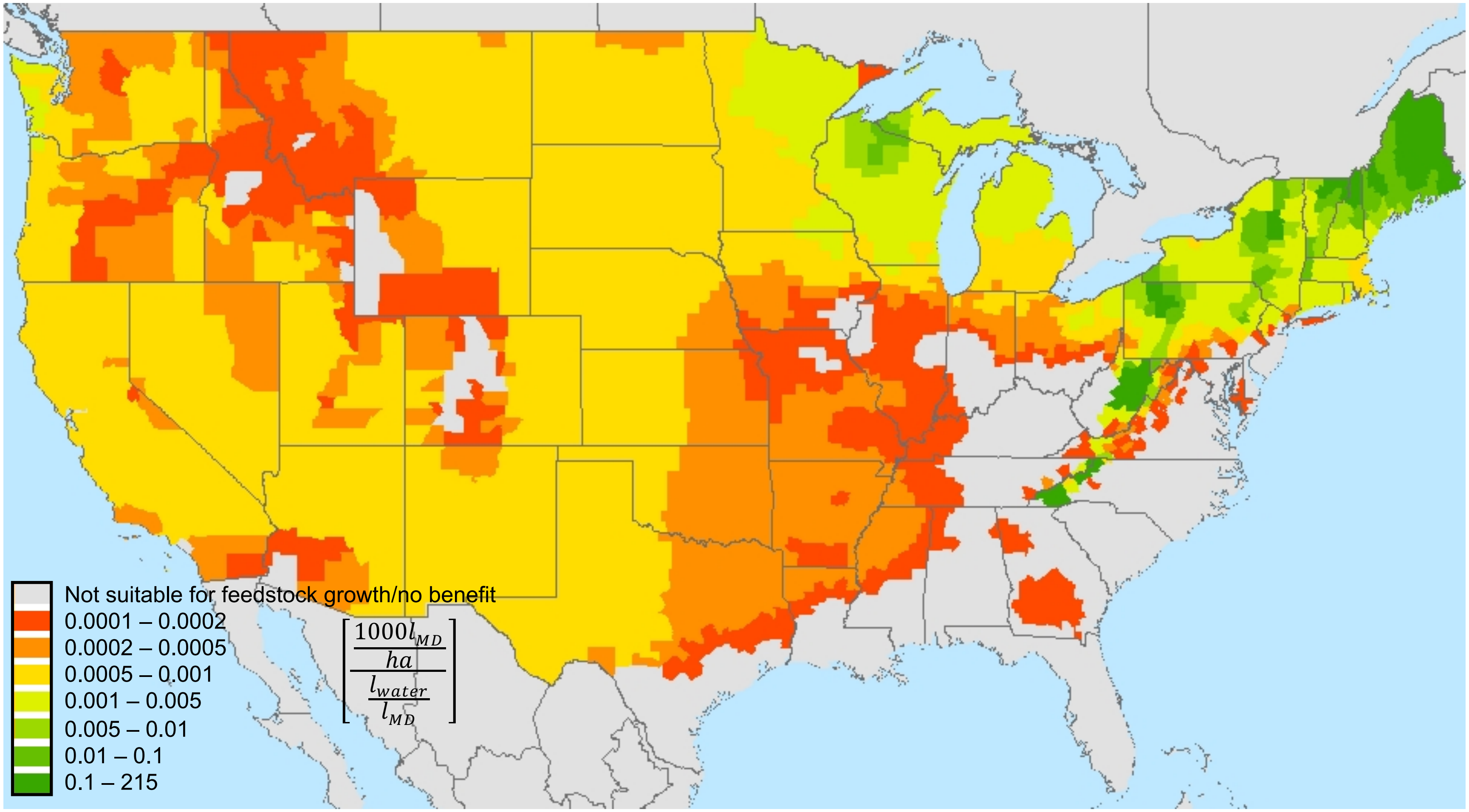

Figure S23: Areal productivity benefit of irrigation for switchgrass AF MD production. $[\frac{\frac{1000 l_{MD}}{ha}}{\frac{l_{water}}{l_{MD}}}]$

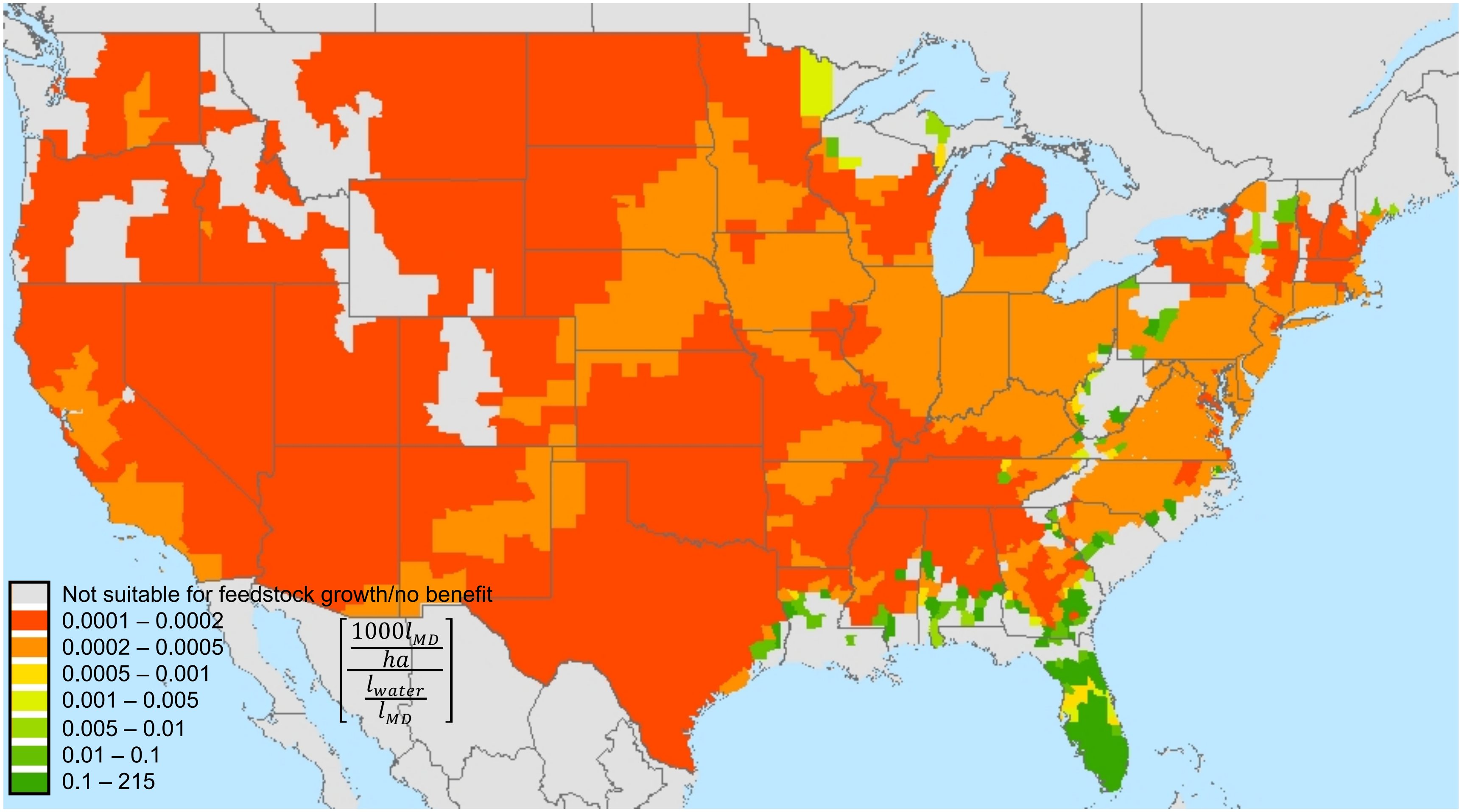

Figure S24: Areal productivity benefit of irrigation for soybean HEFA MD production. $[\frac{\frac{1000 l_{MD}}{ha}}{\frac{l_{water}}{l_{MD}}}]$

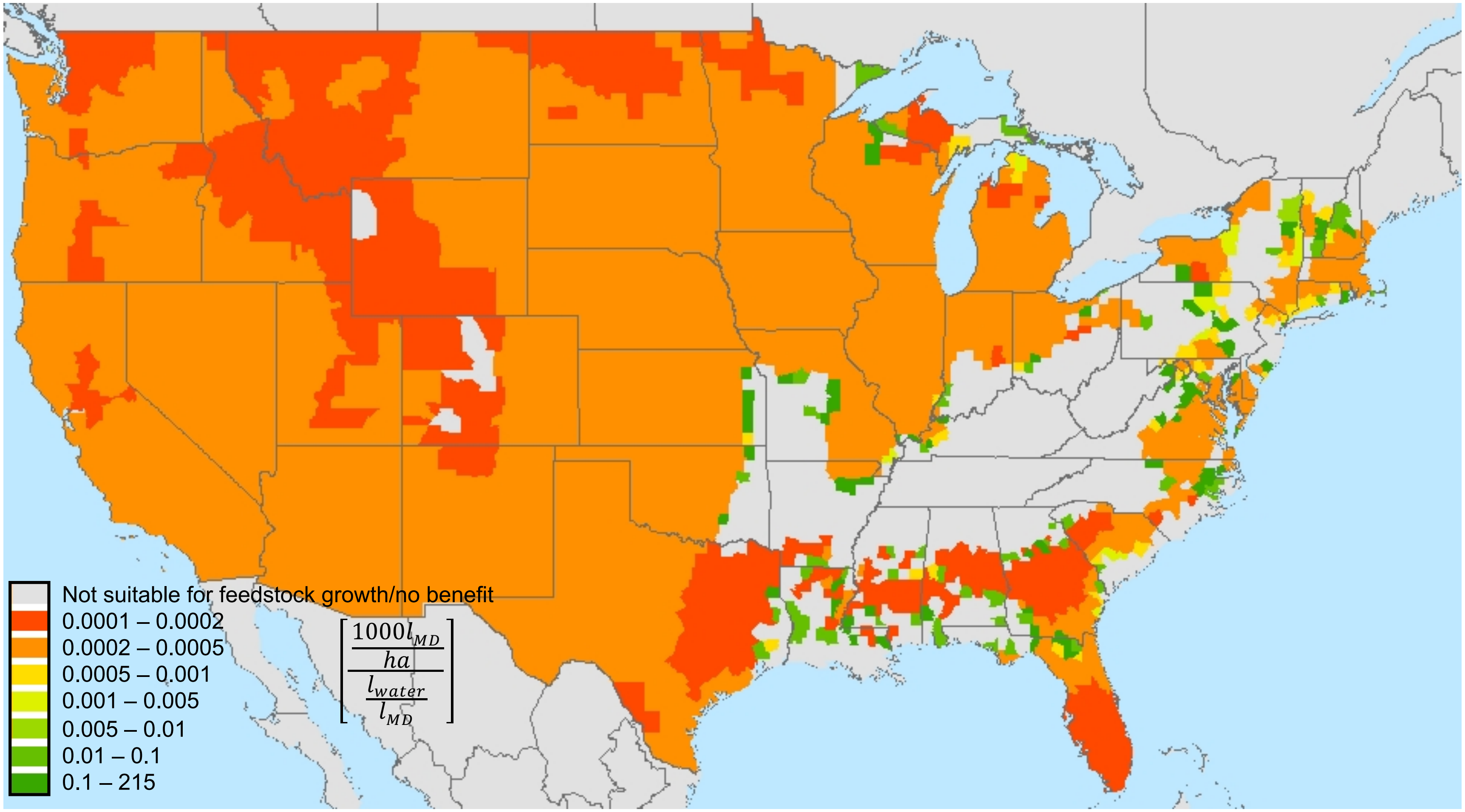

Figure S25: Areal productivity benefit of irrigation for rapeseed HEFA MD production. $[\frac{\frac{1000 l_{MD}}{ha}}{\frac{l_{water}}{l_{MD}}}]$

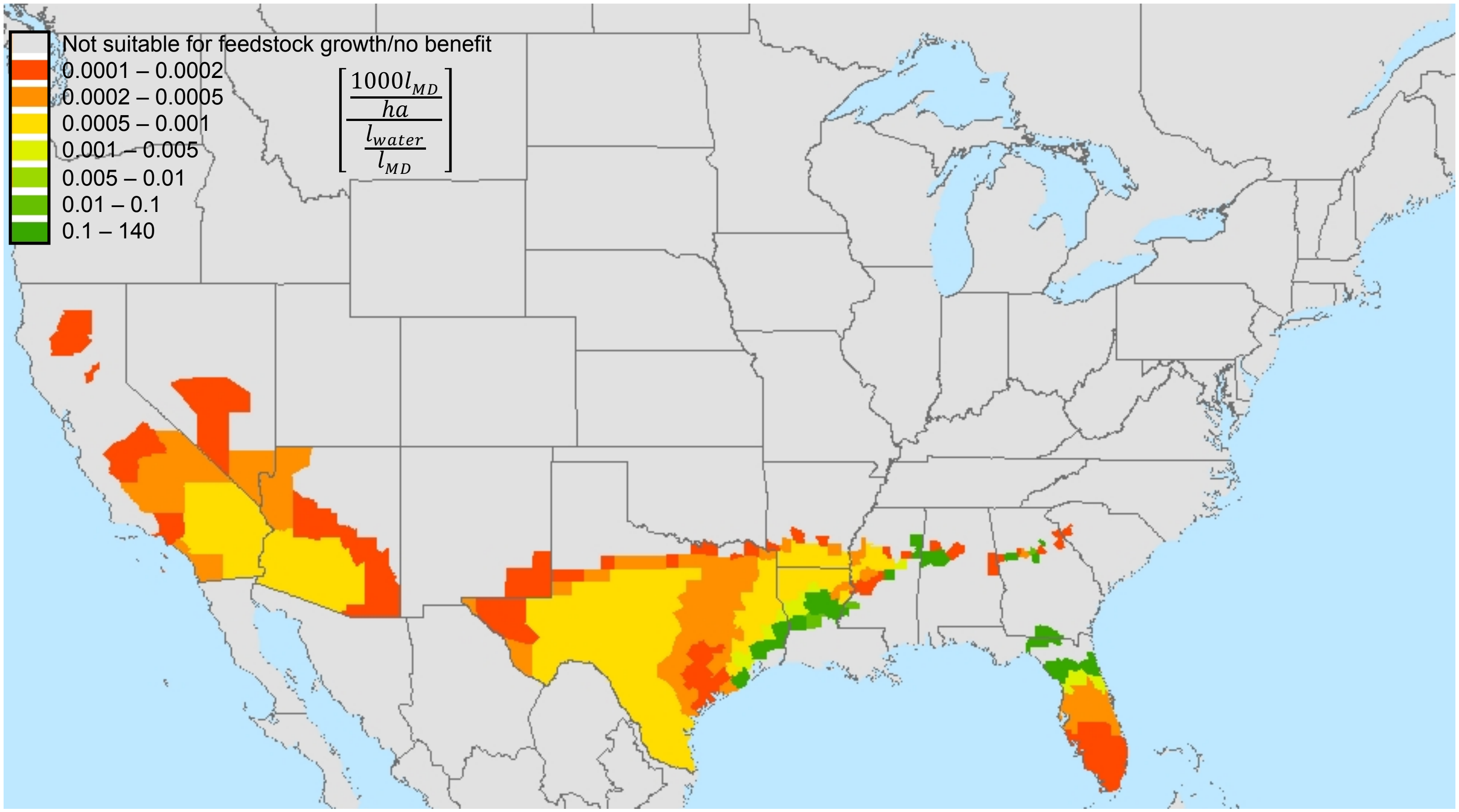

Figure S26: Areal productivity benefit of irrigation for jatropha HEFA MD production. $[\frac{\frac{1000 l_{MD}}{ha}}{\frac{l_{water}}{l_{MD}}}]$

References

[1] Fischer, G.; Nachtergaele, F. O.; Prieler, S.; Teixeira, E.; Toth, G.; van Velthuizen, H.; Verelst, L.; Wiberg, D. Global Agro-ecological Zones (GAEZ v3.0) – Model documentation; International Institute for Applied Systems Analysis: Laxenburg, Austria, 2009.

[2] International Institute for Applied Systems Analysis, Global Agro-ecological Zones (GAEZ v3.0), 2012; http://www.gaez.iiasa.ac.at/w.

[3] Mitchell, T. D.; Jones, P. D. An improved method of constructing a database of monthly cimate observations and associated high-resolution grids. *International Journal of Climatology*, **2005**, 25, 693–712.

[4] United Nations Food & Agricultural Organization, Soil Map of the World, 1974; http://www.fao.org/fileadmin/templates/nr/images/resources/images/SoilMap_hires.pdf.

[5] Consultative Group on International Agricultural Research - Consortium for Spatial Information, Shuttle Radar Topography Mission, 2006; http://srtm.csi.cgiar. org/.

[6] European Commission – Joint Research Comission, Global Land Cover 2000, 2006; http://bioval.jrc.ec.europa.eu/products/ glc2000/products.php.

[7] International Food Policy Research Institute, Global Agricultural Extent v2.0, 2002; http://www.asb.cgiar. org/BNPP/phase2/bnpp_phase2_datasets.htm.

[8] US Geological Survey, Global Land Cover Characteristics Database version 2.0, 2001; http://edcdaac. usgs.gov/glcc/glcc.html.

[9] Earth Resources Observation and Science Data Center, Global Land Survey, 2000; http://eros.usgs.gov/#/Find_Data/ Products_and_Data_Available/GLS.

[10] UN Food and Agricultural Organization, Global Forest Resources Assessment, 2000; http://www.fao.org/forestry/ 32203/en/.

[11] UN Food and Agricultural Organization, Global Forest Resources Assessment, 2005; http://www.fao.org/forestry/ fra/fra2005/en/.

[12] Siebert, S.; Doell, P.; Feick, S.; Hoogeveen, J.; Frenken, K. Global Map of Irrigation Areas, 2007; http://www.fao.org/nr/water/aquastat/irrigationmap/index10.stm.

[13] United Nations Environmental Programme – World Conservation Monitoring Centre, Protected Areas Inventory. 2007; http://www.unepwcmc.org.

[14] Oak Ridge National Laboratory, LandscanTM Global Population Database, 2003; http://www.ornl.gov/landscan/

[15] Fischer, G.; van Velthuizen, H.; Shah, M.; Nachtergaele, F. O. Global Agro-ecological Assessment for Agriculture in the 21st Century: Methodology and Results; International Institute for Applied Systems Analysis: Laxenburg, Austria, 2002.

[16] UN Food and Agricultural Organization, GAEZ Frequently Asked Questions, 2013; http://www.fao.org/nr/gaez/ faqs/en/.

[17] Masutomi, Y.; Takahashi, K.; Harasawa, H.; Matsuoka, Y. Impact assessment of climate change on rice production in Asia in comprehensive consideration of process/parameter uncertainty in general circulation models. *Agriculture, Ecosystems & Environment*, **2009**, 131 (3), 281–291.

[18] Wackernagel, M.; Schulz, N. B.; Deumling, D.; Linares, A. C.; Jenkins, M.; Kapos, V.; Mon- freda, C.; Loh, J.; Myers, N.; Norgaard, R.; Randers, J. Tracking the ecological overshoot of the human economy. *Proceedings of the National Academy of Sciences of the United States of America*, **2002**, 99 (14), 9266–71.

[19] Molden, D., Ed. *Water for Food, Water for Life*; International Water Management Institute, 2007.

[20] Deininger, K.; Byerlee, D.; Lindsay, J.; Norton, A.; Selod, H.; Stickler, M. *Rising Global Interest in Farmland: Can it yield sustainable and equitable benefits?*; The World Bank, 2011.

[21] Gleick, P. Water and Energy, *Annual Review of Energy and the Environment*, **1994**, 19, 267–299.

[22] Gerbens-Leenes, W.; Hoekstra, A. Y.; van der Meer, T. H. The water footprint of bioenergy. *Proceedings of the National Academy of Sciences of the United States of America*, **2009**, 106, 10219–23.

[23] King, C. W.; Webber, M. E. Water intensity of transportation. *Environ. Sci. & Technol.*, **2008**, 42, 7866–72.

[24] US Energy Information Administration, Natural gas production by source, 1990-2040, 2011; http://www.eia.gov/ forecasts/aeo/excel/fig91_data.xls.

[25] Speight, J. G. *The Chemistry and Technology of Petroleum*, 4th ed; CRC Press, 2007.

[26] Wu, M.; Mintz, M.; Wang, M.; Arora, S. Consumptive Water Use in the Production of Ethanol and Petroleum Gasoline; Argonne National Laboratory: Lemont, IL, 2009.

[27] Argonne National Laboratory, Greenhouse Gases, Regulated Emissions, and Energy Use in Transportation (GREET) Model, 2011; http://greet.es.anl.gov/.

[28] Scown, C. D.; Horvath, A.; McKone, T. E. Water foorprint of U.S. Transportation Fuels. *Environ. Sci. & Technol.* **2011**, 45, 2541–53.

[29] Wang, M.; Lee, H.; Molburg, J. Allocation of Energy Use in Petroleum Refineries to Petroleum Products: Implications for Lifecycle Energy Use and Emission Inventory of Petroleum Transportation Fuels, *International Journal of Life cycle Assessment*, **2004**, 9(1), 34–44; DOI 10.1065/lca2003.07.129

[30] Stratton, R. W.; Wong, H. M.; Hileman, J. I. Quantifying variability in life cycle greenhouse gas inventories of alternative middle distillate transportation fuels. *Environ. Sci. & Technol.* **2011**, 45 (10), 4637–44; DOI 10.1021/es102597f

[31] Mielke, E.; Anadon, L. D.; Narayanamurti, V. Water Consumption of Energy Resource Extraction, Processing, and Conversion; Harvard Kennedy School Belfer Center for Science and International Affairs Energy Technology Innovation Policy Research Group: Cambridge, MA, 2010; http://belfercenter.ksg.harvard.edu/files/ETIP-DP-2010-15-final-4.pdf

[32] Bao, B.; El-Halwagi, M. M.; Elbashir, N. O. Simulation, integration and economic analysis of gas-to-liquid processes, *Fuel Processing Technology*, **2010**, 91, 703–713; DOI 10.1016/j.fuproc.2010.02.001

[33] Mantripragada, H. C. Techno-economic evaluation of coal-to-liquids (CTL) plants and their effects on environment and resources. Ph.D. Dissertation, Carnegie-Mellon University, Pittsburgh, PA, 2010.

[34] Dias, M. O.; Ensinas, A. V.; Nebra, S. a.; Maciel Filho, R.; Rossell, C. E.; Maciel, M. R. W. Production of bioethanol and other bio-based materials from sugarcane bagasse: Integration to conventional bioethanol production process, *Chemical Engineering Research and Design*, **2009**, 87(9), 1206–1216; DOI 10.1016/j.cherd.2009.06.020

[35] Ensinas, A. V.; Nebra, S. a.; Lozano, M. a.; Serra, L. M. Analysis of process stream demand reduction and electricity generation in sugar and ethanol production from sugarcane, *Energy Conversion and Management*, 2007, 48(11), 2978–2987; DOI 10.1016/j.enconman.2007.06.038

[36] Lobo, P. C.; Jaguaribe, E. F.; Rodrigues, J.; da Rocha, F. A. A. Economics of alternative sugarcane milling options, *Applied Thermal Engineering*, 2007, 27, 1405–1413; DOI 10.1016/j.applthermaleng.2006.10.023

[37] Macedo, I. d. C., Ed. *Sugar Cane's Energy*, 2nd ed.; Uniao da Indu´stria de Cana-de-Acu´car (Brazilian Sugarcane Industry Association), 2007.

[38] Ethanol Benchmarking and Best Practices; University of Minnesota, Minnesota Technical Assistance Program: Minneapolis, MN, 2008.

[39] Kwiatkowski, J. R.; McAloon, A. J.; Taylor, F.; Johnston, D. B. Modeling the process and costs of fuel ethanol production by the corn dry-grind process*, Industrial Crops and Products* 2006, 23(3), 288–296; DOI 10.1016/j.indcrop.2005.08.004

[40] Mei, F. Mass and Energy Balance for a Corn-to-Ethanol Plant. Masters thesis, Washington University, Saint Louis, MO, 2006.

[41] Mueller, S. Detailed Report: 2008 National Dry Mill Corn Ethanol Survey; University of Illinois at Chicago, Chicago, IL, 2010.

[42] Phillips, S.; Aden, A.; Jechura, J.; Dayton, D. Thermochemical Ethanol via Indirect Gasification and Mixed Alcohol Synthesis of Lignocellulosic Biomass; National Renewable Energy Laboratory, Golden, CO, 2007.

[43] Shapouri, H.; Duffield, J. A.; Wang, M. The Energy Balance of Corn Ethanol: An Update; United States Department of Agriculture, Washington, DC, 2002.

[44] Wang, M.; Wu, M.; Huo, H. Lifecycle energy and greenhouse gas emission impacts of different corn ethanol plant types, *Environmental Research Letters*, 2007, 2(2), 1-13; DOI 10.1088/1748-9326/2/2/024001

[45] Aden, A.; Ruth, M.; Ibsen, K.; Jechura, J.; Neeves, K.; Sheehan, J.; Wallace, B.; Montague, L.; Slayton, A.; Lukas, J. Lignocellulosic Biomass-to-Ethanol Process Design and Economics Utilizing Co-current Dilute Acid Prehydrolysis and Enzymatic Hydrolysis for Corn Stover; National Renewable Energy Laboratory, Golden, CO, 2002.

[46] Humbird, D.; Davis, R.; Tao, L.; Kinchin, C.; Hsu, D.; Aden, A. Process Design and Economics for Biochemical Conversion of Lignocellulosic Biomass to Ethanol; National Renewable Energy Laboratory, Golden, CO, 2011.

[47] Kumar, D.; Murthy, G. S. Impact of pretreatment and downstream processing technologies on economics and energy in ethanol production, *Biotechnology for biofuels*, **2011**, 4(10), 27; DOI 10.1186/1754-6834-4-27

[48] Najafpour, G. D. *Biochemical Engineering and Biotechnology*; Elsevier B.V., 2007.

[49] Staples, M. D. Personal communication with Hussain Abidi, Post-doc at MIT. Email, 2012.

[50] Staples, M. D. Personal communication with Kevin Weiss, CEO Byogy. Email, 2012.

[51] Staples, M. D. Personal communication with Glenn Johnston, VP Gevo. Email, 2012.

[52] Staples, M. D. Personal communication with Wei Huang, VP LS9. Email, 2012.

[53] Carter, N. A. Environmental and Economic Assessment of Microalgae-derived Jet Fuel. Master's thesis, Massachusetts Institute of Technology, Cambridge, MA, 2012.

[54] Vaswani, S. Biodiesel from Algae; SRI Consulting, Menlo Park, CA; 2009.

[55] Pearlson, M.; Wollersheim, C.; Hileman, J.; August, R. A techno-economic review of hydroprocessed renewable esters and fatty acids for jet fuel production, *Biofuels, Bioproducts and Biorefining* **2013**, 7, 89–96; DOI 10.1002/bbb.1378

[56] Sheehan, J.; Camobreco, V.; Duffield, J.; Graboski, M.; Shapouri, H. Life Cycle Inventory of Biodiesel and Petroleum Diesel for Use in an Urban Bus; National Renewable Energy Laboratory, Golden, CO, 1998.

[57] Wang, M.; Huo, H.; Arora, S. Methods of dealing with co-products of biofuels in lifecycle analysis and consequent results with the U.S. context. *Energy Policy*, **2011**, 39 (10), 5726–5736; DOI 10.1016/j.enpol.2010.03.052

[58] United States Grain Council, 2012;
http://www.grains.org/images/DDGS%20Weekly%20Reports/USGC%20-%20DDGS%20Weekly%20Market%20Report%20August%203.2012.pdf.

[59] US Energy Information Administration, 2012; http://www.eia.gov/electricity/monthly/epm_table_grapher.cfm?t=epmt_5_6_a.

[60] Independent Chemical Information Service, 2012; http://www.icispricing.com/.

[61] Bailis, R. E.; Baka, J. E. Greenhouse gas emissions and land use change from jatropha Curcas-based Jet Fuel in Brazil. *Environ. Sci. & Technol.*, 2010, 44, 8684–91.

[62] Donnis, B.; Egeberg, R. G.; Blom, P.; Knudsen, K. G. Hydroprocessing of bio-oils and oxygenates to hydrocarbons. Understanding the reaction routes. *Topics in Catalysis,* 2009, 52, 229–240.

[63] Huo, H.; Wang, M.; Bloyd, C.; Putsche, V. Life-cycle assessment of energy and greenhouse gas effects of soybean-derived biodiesel and renewable fuels, *Environ. Sci. & Technol.*, 2009, 43, 750–6.

[64] Honeywell UOP, Controlling Production of Transportation Fuels from Renewable Feedstocks. Patent: WO 2009/151692 A2, 2009.